



## A multi-objective sustainable multipath delivery problem in hilly regions with customer-satisfaction using TLBO

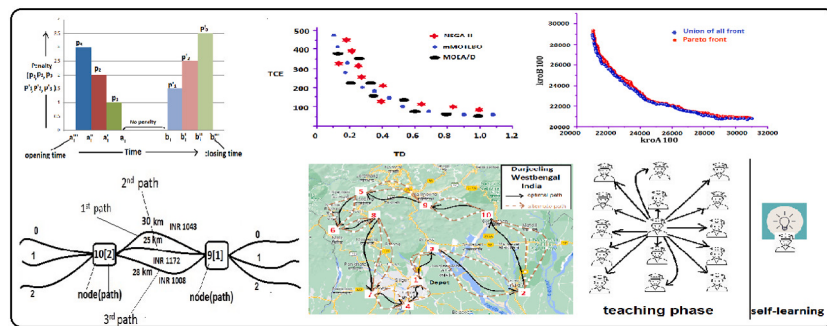
Somnath Maji <sup>a</sup>, Samir Maity <sup>b</sup>\*, Izabela Ewa Nielsen <sup>b</sup>, Debasis Giri <sup>c</sup>,  
Manoranjan Maiti <sup>b</sup>

<sup>a</sup> Department of Computer Science & Engineering, Maulana Abul Kalam Azad University of Technology, Nadia 741249, W.B., India

<sup>b</sup> Department of Materials and Production, Artificial Intelligence for Operations Research (AI4OR) Group, Aalborg University, 9220, Aalborg, Denmark

<sup>c</sup> Department of Information Technology, Maulana Abul Kalam Azad University of Technology, Nadia 741249, W.B., India

### GRAPHICAL ABSTRACT



### ARTICLE INFO

#### Keywords:

Sustainable development goal  
Sustainable logistic routing  
Hilly road network  
Customer satisfaction  
MOTLBO

### ABSTRACT

Logistic delivery through road contributes substantial carbon emission (CE). In business, timely goods delivery i.e. customer satisfaction, is important. With these facts, a sustainable multi-objective 3D delivery problem with customer satisfaction (SMO3DDPwCS) in a hilly region (HR) is developed to minimize total CE and customer dissatisfaction (CDS) simultaneously. Here, one supplier's vehicle starts from the depot with goods equal to retailers' demands, distributes among the retailers as per their orders within their preferred times, and comes back. The retailers' shops and depot are connected through multiple hilly tracks, which have up and down slopes and are susceptible to landslide. The cautious driving through these tracks produces extra CE and CDS. The SMO3DDPwCS is solved by a modified MOTLBO (mMOTLBO) algorithm. This algorithm incorporates self-learning concepts after both the teaching and learning phases, introduces innovative upgrading strategies, and employs a group-based learning approach. Some statistical tests are performed using mMOTLBO on the standard TSPLIB instances. The efficiency of mMOTLBO is established against NSGA-II and MOEA/D. Multiple solutions in Pareto front are ranked using TOPSIS. Some managerial decisions are drawn. The optimum routing plan for SMO3DDPwCS in a hilly region is presented and gives better results (31% total CE and 8% total CDS) than the single path formulation. mMOTLBO showed superiority over other algorithms in most cases concerning the Pareto front for the objectives. On the benchmark instances, mMOTLBO demonstrated its superiority by outperforming NSGA-II and MOEA/D, showing improvements of 0.11 in IGD and 4.12 in GD.

\* Corresponding author.

E-mail addresses: [somnathmajivucs@gmail.com](mailto:somnathmajivucs@gmail.com) (S. Maji), [samirm@mp.aau.dk](mailto:samirm@mp.aau.dk) (S. Maity), [izabela@mp.aau.dk](mailto:izabela@mp.aau.dk) (I.E. Nielsen), [\(D. Giri\)](mailto:mmaiti2005@yahoo.co.in), [\(M. Maiti\)](mailto:debasis_giri@hotmail.com).

## 1. Introduction

### 1.1. Motivation

The Sustainable Development Goals (SDGs) [1] are a collection of 17 international objectives that were approved by the United Nations<sup>1</sup> in order to address global challenges of social, economic, and environmental sustainability. One of the important issues is to mitigate the climate change<sup>2</sup> and carbon emissions throughout the world. The logistic transportation has a huge impact on global greenhouse gas (GHG) emission<sup>3</sup> whereas UN's objective is zero-emission by 2050. Thus logistic delivery system needs special attention to meet the challenges [2]. In the last decade, several researchers are engaged to achieve the SDG with respect to (wrt) carbon emission in road transportation. Logistic routing in a landslide-prone hilly region [with multiple path connections among two places has not been extensively] investigated. This process involves (i) road gradient, (ii) unpredictable landslides, (iii) nature of the soil, (iv) road restoration time, etc. The present investigation focuses on the above issues.

To reduce transportation's environmental impact, we study fuel minimization in logistics transportation sectors. Minimization of fuel consumption drastically reduces carbon footprints. Researchers studied route optimization, vehicle load balancing, fuel-efficient technologies, and alternative energy sources to reduce carbon emissions and improve logistic transportation [3]. This research presents a sustainable road transportation system finding the optimum routing path in a hilly region (HR) for minimum carbon emission (CE).

Nowadays, in the competitive business world, suppliers opt for customer-oriented services. Customer's discontent [4] impact on transportation systems performance motivates us to study dissatisfaction minimization. Dissatisfied customers can cause negative word-of-mouth, lower supplier loyalty, and financial losses for the suppliers. So, the research work on a more customer-centric transportation system i.e. discontent minimization is preferable. Here nonlinear penalty costs for consumer dissatisfaction wrt delivery time are assumed to represent a real-life situation.

Understanding how road gradient affects transportation efficiency and cost/time optimization is essential in hilly regions [5]. The slope of a road affects fuel consumption, vehicle performance, and transportation cost/time. Vehicles use more fuel and incur higher operating costs/times on steep paths. Researchers study road gradients and transportation logistics to find optimal route planning, load distribution, and vehicle selection strategies that reduce fuel consumption and transportation costs. The present research helps to create energy-efficient transport systems, to minimize carbon emissions, and to make logistics operations more profitable.

With the infrastructural development, nowadays, there are several connecting routes between two different places. A minimum distance path may not always yield the best results for logistic transportation. Because these routes are different, some are shorter but congested, good but have many toll plazas, etc. These characteristics lead to different CE amounts, costs, and times during transportation. Recently, assuming multipath connections between different places, Maji et al. [6] and Thakur et al. [7] presented purchaser and delivery problems for sustainable and resilient transportation networks.

For efficient and effective decision-making in a sustainable logistic transportation (delivery) system, minimization of CE and customers' dissatisfaction (CDS) is required. These objectives are contradictory to each other and ultimately, a compromise solution is obtained. This prompted us to formulate a multi-objective problem and to develop an

appropriate optimization method for this purpose. The multi-objective routing problems are NP-hard problems, which are normally solved by metaheuristic methods. Several researchers [8] have used the multi-objective teaching learning based optimization (MOTLBO) in different areas. This motivated us to develop the appropriate modified MOTLBO (mMOTLBO) for the present multi-objective logistic routing system. The TLBO algorithm is inspired by the teaching learning process in a classroom. In this study, we introduce the concept of self-learning after both the teaching and learning phases, along with novel upgradation strategies and group-based learning [9]. This research will help decision-makers to balance the conflicting objectives and to make logistics routing decisions that improve cost-effectiveness, customer satisfaction, and environmental performance.

The following relevant questions arise in connection with the above supplier's distribution problem for minimum CE and CDS.

### 1.2. Research questions

Q1: How the nodes (retailer's shops) will be selected to reduce CDS in multipath routing?

Q2: How to meet the minimum emission in three dimensional (3D) logistic routing in HR?

Q3: What influence does road gradient have on energy use and transportation effectiveness, and how can it be optimized for environmentally friendly and economically viable transportation systems?

Q4: How to establish a multipath transport system to improve the effectiveness, resilience, and sustainability of logistic transport, and what are the advantages and difficulties associated with it?

Q5: What are the elements that lead to CDS and corresponding penalty charges? How they can be reduced to increase customer satisfaction, to lessen financial losses, and to boost overall transportation performance?

Q6: How can decision-making processes be optimized to achieve a balance between competing objectives like reducing CE and minimizing CDS in transportation planning and management? What are the key considerations and methodologies for solving this multi-objective logistic routing problem?

Q7: How to develop an appropriate mMOTLBO to solve the sustainable multi-objective 3D delivery problem with customer satisfaction (SMO3DDPwCS)?

To answer the above questions, we developed an SMO3DDPwCS in HR and solved by mMOTLBO developed for this purpose. In the proposed model, in a hilly region, a supplier's vehicle with an amount of an item, which is equal to the sum of the demands of the retailers having shops (node) at different places starts from the depot, tries to deliver the goods at the retailers' shops during their preferred time as per their demand, and comes back to the depot. There are different connecting paths among the shops and between the depot and shops. The hill tracks are of ups and downs in nature having different curvatures. In this process, some CE is emitted and the supplier faces CDS as it may not be possible to deliver during the preferred times of all retailers. Thus, the problem is to find the optimum routing path for minimum CE and CDS. To solve this multi-objective, a mMOTLBO with Probabilistic selection, a novel up-gradation technique in the teaching phase with self-learning, and interactive group-based crossover for learners in the learning phase with self-learning is developed. To prove its effectiveness, some benchmark instances from TSPLIB [10] are solved. Statistical tests are also performed to establish mMOTLBO's superiority.

Novelties in this investigation are:

- For the first time in the literature, a multipath routing problem in a hilly region with its characteristics (ups and down, landslide, etc.) is formulated.
- Sustainable multi-objective multipath delivery problem for minimum CDS and CE in hilly regions is developed.

<sup>1</sup> <https://sdgs.un.org/goals>

<sup>2</sup> <https://sdgs.un.org/goals/goal13>

<sup>3</sup> <https://www.epa.gov/greenvehicles/fast-facts-transportation-greenhouse-gas-emissions>

- Non-linear penalty cost due to customer dissatisfaction is considered.
- Road gradient, estimation of landslide occurrence and landslide debris recovery time are derived and effects of these are considered on vehicle's traveling.
- For the solution of a multi-objective problem, a modified MOTLBO is developed and applied. Its supremacy is established through statistical tests. Novel teaching techniques, group-based learning techniques with self-learning, and probabilistic selection are used in the proposed mMOTLBO, which can be used in the multi-objective optimization problems in other areas such as traveling purchaser problem (TPP), traveling salesman problem (TSP), facility location problem, etc.
- Efficiency of mMOTLBO is established against Non-dominated sorting genetic algorithm (NSGA-II) and Multi-objective evolutionary algorithm based on decomposition (MOEA/D).

The paper is organized as follows: In Sections 1 and 2, a concise introduction with motivation and a brief literature review respectively are given. Section 3 gives some mathematical formulation of SMO3DDPwCS models. The proposed algorithm is explained in Section 4. The validity of the proposed algorithm is presented in Section 5. Some real-life experiments and a brief discussion on experimental results are found in Section 6. Some managerial discussions are presented in Section 7. Finally, a conclusion and future scope are available in Section 8.

## 2. Background and literature review

### 2.1. Model related

#### 2.1.1. Fuel consumption

The price of fuel is a significant consideration in any transportation problem. There have been numerous investigations [11], focusing on fuel consumption in the context of routing problems. These investigations aim to optimize routing decisions to minimize fuel consumption, considering factors such as vehicle characteristics, road conditions, traffic patterns, and load constraints. The study conducted by Micheli and Mantella [12] proposes a hypothesis that the quantity of fuel consumption in a routing problem is influenced by several factors, including the type of vehicle, vehicle velocity, the weight of the transported items (including the vehicle's own weight), and the weight of the transported products, etc. The present investigation is following Micheli and Mantella [12] proposed hypothesis.

#### 2.1.2. Road gradient

Though a few studies have attempted [5,13] to consider the road gradients when calculating fuel consumption, none of them have attempted to account for actual road gradients over the whole road network while formulating the transportation model. This has inspired us to take into account the actual road slopes in order to more accurately estimate fuel usage. Thus our study aims to incorporate realistic road gradients, vehicle-specific features, and arc-based speeds to estimate energy requirements effectively.

#### 2.1.3. Carbon emission

In recent years, much research has focused on reducing carbon emissions due to logistical activities. Scora and Barth [14] presented comprehensive emission models for heavy-duty diesel cars' fuel consumption and the accompanying carbon emissions. These comprehensive models were further utilized in a variety of vehicle routing problems (VRPs) to assess fuel consumption by Bektaş and Laporte [15]. A bi-objective fuel-efficient green VRP with variable speed limitations was developed by Comert and Yazgan [16]. In order to obtain non-dominant solutions, a hybrid strategy was utilized. This approach was

developed using an alternating locate-allocate heuristic and neutrosophic compromise programming as its foundation. Sabet and Farooq [11] solved an eco-friendly VRP taking into account urban congestion. A green four-dimensional (4D) transport problem with fixed charge, carbon emission, transport cost, and time was solved by Giri and Roy [17] using neutrosophic and Pythagorean hesitant fuzzy programming.

#### 2.1.4. Customer satisfaction/dissatisfaction

Ren et al. [18] investigated a multi-center joint distribution optimization model as a vehicle routing problem with time windows (VRPTW) considering the distribution cost, carbon emissions, and customer satisfaction and solved by enhanced Ant Colony technique. They considered two types of time window-acceptable time windows and satisfied time windows. They did not consider penalty costs due to customer dissatisfaction. In this investigation, we consider non-linear costs for this. Wang et al. [19] examined a bi-objective vehicle-routing problem that involves soft time windows and multiple depots. The objective is to minimize both total energy consumption and customer dissatisfaction simultaneously. They employed the  $\epsilon$ -constraint method and NSGA-II (Non-dominated Sorting Genetic Algorithm II). Wang et al. [20] examined cost-effective vehicle scheduling for perishable goods by maximizing customer satisfaction. Here freshness and delivery timing determine customer happiness. A multi-objective vehicle scheduling optimization model for perishable products maximizes customer happiness and minimizes delivery costs based on priority. They did not consider penalty costs due to customer dissatisfaction. There are some investigations [21] available in the literature on customer dissatisfaction.

#### 2.1.5. Landslide

Wijaya et al. [22] investigated high-resolution 1 km x 1 km down-scaled extreme rainfall estimates for multiple time periods and scenarios. The baseline (1976–2005) and future (2030s, 2050s, and 2080s) Representative concentration pathways (RCP) 4.5 and 8.5 scenarios are included. Using extreme rainfall estimates, they presented and analyzed landslip susceptibility maps using frequency ratio (FR) and analytical hierarchy process (AHP) methods. Throughout the four RCP scenarios, nine multivariate elements were analyzed for their contribution to landslides. These elements included terrain slope, elevation, lithology, soil, distances from lineaments, and streams, land use, and mean annual rainfall. Hafsa et al. [23] investigated regional landslip susceptibility maps for the Chittagong Hilly Areas (CHA) in Bangladesh using the FR method with two approaches: the analytical hierarchy process and logistic regression. Chen and Lee [24] introduced a quasi-three-dimensional model based on the Lagrangian finite element method to simulate the dynamic run-out process resulting from landslides. The model aims to accurately reproduce the movement and behavior of landslides in a realistic manner. Khoroshilov et al. [25] investigated modeling anthropogenic landslip slope movements. They studied how different factors affect landslip point vertical displacements. These findings enable more detailed qualitative descriptions of circumstances.

#### 2.1.6. Delivery problem

Ben-Said et al. [26] investigated decomposing the search space into numerous linearly aggregated sub-problems, yielding a two-phase framework to solve selective pickup and delivery problems with time windows. Local search with specific removal and insertion operators optimizes aggregated problems. Lu et al. [27] explored the application of a truck and drone cooperative delivery model in humanitarian logistics. They introduced a multi-objective humanitarian pickup and delivery vehicle routing problem with drones that consists of cooperative routing and relief supplies allocation subproblems. The authors employed hybridized ant colony optimization (HACO) algorithm to solve this problem. Ghasemi et al. [28] investigated a two-objective mathematical location-routing model that minimizes expenses and maximizes dependability to deliver goods to customers on time within

the predicted time and time window. In small, medium, and large-size problems, Epsilon-constraint and NSGA-II were used to solve the mathematical model.

Some multipath investigations are done for single objective routing type problems [6,7]. But none considered multipath in the multi-objective routing problem.

## 2.2. Solution methods related

### 2.2.1. Metaheuristic algorithm

Due to the NP-hard nature of TSP, solving it directly becomes challenging. As a result, various metaheuristic algorithms, such as Genetic Algorithm (GA) [29], Ant Colony Optimization [30], Fireworks Algorithm [31], Particle Swarm Optimization [32], is employed to address this type of problems effectively. Recently, Rao et al. [33] introduced a novel metaheuristic optimization algorithm called teaching learning based optimization (TLBO), inspired by the process of teaching and learning. TLBO consists of two main phases: teaching phase and learning phase. During the teaching phase, learners aim to enhance their performance by drawing from the teacher's expertise and learning from their peers. In practice, learners cannot focus on all subjects equally and consistently compete with their peers. To address these aspects, we have designed TLBO in such a way that learners upgrade themselves differently across various subjects during the teaching phase. Additionally, a group-based learning strategy is employed to foster interactions and improve learners' performance during the learning phase. TLBO has been used mostly in continuous optimization problems [8,34,35]. However, a few researchers have also applied TLBO to combinatorial optimization problems [36]. Li et al. [36] explored the application of discrete TLBO in solving flow-shop rescheduling problems. They presented the canonical form of TLBO and updated the learner through teaching phase-I, II, and learning phase-I, II. Furthermore, they employed the IG-local search technique and repaired newly generated learners for upgradation.

While most investigations focus on using the mean of the class for upgrading learners during the teaching phase, our study takes a different approach by considering individual differences between the learner and teacher. We upgrade the learner uniquely for various subjects to address this aspect effectively. In the learning phase, learners interact among themselves and are always in a competitive state. To improve the learners during this phase, we introduce a novel interactive group-based crossover method, where learners are randomly selected to form groups, ensuring population diversity. The combination of these two phases allows us to strike a good balance between exploration and exploitation within TLBO, enhancing its overall performance.

### 2.2.2. Multi-objective TLBO

In Multi-Objective Generalized Teacher-Learning-Based-Optimization Algorithm, Ram et al. [37] included, numerous teachers in the Teacher phase, and in the Student phase, they added Euclidean distance. In order to generate more varied solutions, they modified TLBO, created a multi-objective form of it, and solved the multi-model problems. In another study by Li et al. [38], a mathematical formulation is presented to balance a multi-objective, two-sided assembly line while considering multiple constraints. They considered the self-learning phase along with the teaching and learning phase to improve multi-objective TLBO. Yang and Liu [39] optimized passive power filters (PPFs) to suppress important harmonics and enhance power factors. TLBO and Pareto optimality address this multi-objective PPF design challenge. The strategy integrates fuzzy decision-making and an external archive. Sub-group search and teacher selection strategies increase non-dominated solution diversity.

All the above problems are mainly focused on continuous, multi-objective problems. For discrete optimization problems, Chen et al. [40] proposed a method for redefining learner representation and updating rules. A multi-objective discrete method (MODTLBO/D) for

community detection in complicated networks is based on the discrete variant, DTLBO. To avoid local optima and maintain population variety, multi-objective decomposition, and neighbor-based mutation are used. Finally, real-world networks are studied to test the method. MODTLBO/D outperforms other community discovery techniques in complicated networks. In their study, Lei and Su [8] explored the Distributed Hybrid Flow Shop Scheduling Problem with sequence-dependent setup times. They introduced a multi-class TLBO approach to address this problem with the objective of minimizing both the makespan and maximum tardiness. Two teacher phases and one learner phase are used to evaluate each class. Elimination of the worst class saves computational resources. They did not solve the benchmark instances for discrete problems from TSPLIB.

This literature survey is presented in concise form in [Table 1](#).

## 2.3. Research gap

From the above history, it is evident that simultaneous optimization of CE and CDS, consideration of penalty cost for CDS, and fixed-charge costs were limited to two-dimensional (2D) logistic routing in plain land where only one route is available connecting the nodes/cities. Earlier researchers did not consider multipath routing, which leads to the questions—Q1, Q2, Q4, Q5, and Q6. Again, none has considered the routing with the characteristics of a hilly region, which generates Q3. For compromise solutions in the multi-objective problem, very few have used MOTLBO in the logistic routing problems. Moreover, some modifications are made in the usual MOTLBO. This leads to Q6 and Q7. The current study addresses to remove the above research gaps.

## 3. Proposed sustainable multi-objective 3D delivery problem with customer satisfaction (SMO3DDPwCS)

### 3.1. Nomenclature

The notations used in this investigation are given in [Table 2](#).

### 3.2. Assumptions/constraints

- (i) The total distributed amount at the nodes is equal to the total demand.
- (ii) The supplier visits a retailer's shop only once and delivers the required amount as per the retailer's order during the retailer's operation time.
- (iii) The supplier starts from a depot with a vehicle having sufficient capacity and returns to the same depot after delivery.
- (iv) The supplier has prior idea/information about the retailers' demands and the shops' operation times.
- (v) Different shops are operated at different time slots in a day, and acceptable time windows are different.
- (vi) If goods are not delivered in the acceptable time window, then a non-linear penalty cost to be paid by the supplier is assigned in favor of retailers.
- (vii) There are several connecting paths (three in this investigation) between the markets and among the markets and depot.
- (viii) The routing area is a hilly area and the paths between the nodes are sloppy tracts, having downward, horizontal, and upward slopes randomly. Thus, every path between two arbitrary nodes is divided into three parts (up, down, and horizontal)
- (ix) Some paths have land slide-prone areas for a certain distance (known from the past records) and there is a Govt. rescue team (like National Disaster Response Force in India), to remove the landslide debris at the earliest if a landslide occurs.
- (x) The velocities (km/hr) of the vehicle are different for different paths and assigned randomly within an interval [10, 35].

**Table 1**  
Literature survey of this investigation.

References	Models	Applied methods	Objective & Constraint	Parameters
Year wise	Variant's of problem	Exact Heuristics Metaheuristics NSGA-II MOEA/D MOTLBO	Cost Time Cost constraint Time constraint Carbon Emission Land slide	Customer dissatisfaction Road gradient Multipath
Molina et al. [41]	Solid multi-objective	✓ ✓ ✓	✓ ✓ ✓	✓
Iqbal et al. [42]	Solid multi-objective	✓ ✓ ✓	✓ ✓ ✓	✓
Li et al. [38]	Multiple multi-objective	✓	✓ ✓	
Toro et al. [43]	Location routing	✓	✓ ✓ ✓	
Micheli and Mantella [12]	multi-objective with multiple vehicle	✓ ✓	✓ ✓	
Eirgash et al. [44]	Capacitated supplier selection		✓ ✓	
Eirgash et al. [44]	multi-objective with quantity discount	✓ ✓	✓ ✓	
Liao et al. [45]	multi-objective with decision hierarchy	✓ ✓	✓	
Yang and Liu [39]	Double multi-objective	✓	✓	
Zajac and Huber [46]	Time-dependent multi-objective	✓ ✓	✓ ✓	
Ram et al. [37]	multi-objective with incompatibility	✓	✓ ✓	
Ren et al. [18]	multi-objective and multi-objective variants	✓ ✓ ✓	✓ ✓ ✓ ✓	✓
Lei and Su [8]	multi-objective with multiple vehicle	✓	✓ ✓	
Pilati and Tronconi [47]	Solid multi-objective		✓ ✓ ✓	
Thakur et al. [7]	Delivery	✓	✓ ✓	
Present investigation (2023)	Delivery	✓ ✓ ✓ ✓ ✓	✓ ✓ ✓ ✓ ✓ ✓ ✓	✓ ✓ ✓

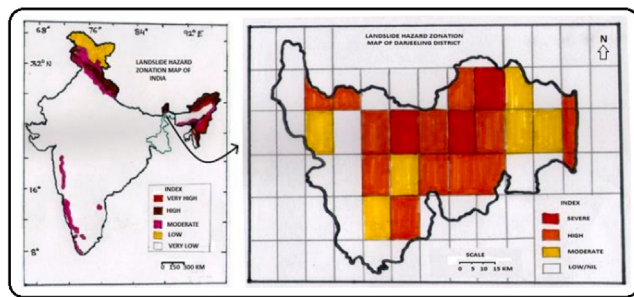


Fig. 1. Landslide Hazard Zonation Map of Darjeeling.

### 3.3. Sustainable multi-objective 3D delivery problem with customer satisfaction (SMO3DDPwCS)

#### 3.3.1. Statement of SMO3DDPwCS

In a hilly area (see Fig. 1), depending on the demands made in advance by the retailers, a supplier with a vehicle carrying goods starts from a depot and returns after dropping the goods off at the retailers' locations (i.e. "nodes") as per the retailers' demand. The dispatched goods meet the demands of all retailers. Between the depot and the retailers, as well as among the retailers, there are various connecting paths. The goods are delivered within the shop's operation times, preferably within the retailer's time windows, known earlier by the supplier. The goods vehicle chooses the optimum routing plan so that total CE and CDS are at a minimum.

#### 3.3.2. Type of hilly tracts and fuel consumption

The vehicle determines a complete tour  $(x_1, x_2, \dots, x_N, x_1)$  with  $r \in R$  routes to deliver goods to the retailers. Following Micheli and

Mantella [12] expression,

$$CE = \sum_{i=1}^{N-1} U \lambda \left[ y \left( \frac{dis(x_{(i)(i+1)}, r)}{v_{(x_{(i)(i+1)}, r)}} \right) + \gamma \beta dis(x_{(i)(i+1)}, r) v^2(x_{(i)(i+1)}, r) \right. \\ \left. + \gamma s \{ \mu + (D - \sum_{t=2}^i d_t) \} dis(x_{(i)(i+1)}, r) + U \lambda \left[ y \left( \frac{dis(x_{(N)(1)}, r)}{v_{(x_{(N)(1)}, r)}} \right) \right. \right. \\ \left. \left. + \gamma \beta dis(x_{(N)(1)}, r) v^2(x_{(N)(1)}, r) + (\gamma s \mu) dis(x_{(N)(1)}, r) \right] \right] \quad (1)$$

Eq. (1) calculates total carbon emission throughout the routing. Here, three different components of the carbon emission function. The first component is the engine module, expressed as  $\lambda(y(\frac{dis(x_{(i)(i+1)}, r)}{v_{(x_{(i)(i+1)}, r)}}))$ , which is linear in travel time. The second component is the speed module, expressed as  $\gamma s \{ \mu + (D - \sum_{t=2}^i d_t) \} dis(x_{(i)(i+1)}, r)$ , which is quadratic in speed. The third component is the weight module, expressed as  $\gamma s \{ \mu + (D - \sum_{t=2}^i d_t) \} dis(x_{(i)(i+1)}, r)$ , and is independent of vehicle speed. The last component includes the  $(D - \sum_{t=2}^i d_t)$  related to the weight carried by the vehicle, linking the routing part of the proposed problem. A heavier vehicle consumes more fuel, leading to higher carbon emissions. These emissions, expressed in  $kgCO2e$ , are obtained by multiplying the fuel consumption by the fuel-dependent conversion factor  $U$ , expressed in  $kgCO2e/litre$ . Here,  $(D - \sum_{t=2}^i d_t)$  determines the remaining amount after visiting  $i$ th node.

Here (see Fig. 2), every path between two arbitrary nodes is divided into three portions randomly, i.e. up, down, and horizontal with different gradients (cf. Figs. 3(a) and 3(b)) through Eq. (2). Here  $dis(x_{(i)(i+1)}, r)$  is distance between  $i$ th to  $(i+1)$ th node using  $r$ th route. Assume this route is divided into three parts, i.e.,  $dis(x_{(i)(i')}, r)$ ,  $dis(x_{(i')(i'')}, r)$ , and  $dis(x_{(i'')(i+1)}, r)$ . Each segment is divided by different velocities to evaluate the travel time, and summing these values provides the total travel time. Similarly, different angles and road slopes are determined through  $\phi$ .

$$\text{where, } \frac{dis(x_{(i)(i+1)}, r)}{v_{(x_{(i)(i+1)}, r)}} = \frac{dis(x_{(i)(i')}, r)}{v_{(x_{(i)(i')}, r)}} + \frac{dis(x_{(i')(i'')}, r)}{v_{(x_{(i')(i'')}, r)}} + \frac{dis(x_{(i'')(i+1)}, r)}{v_{(x_{(i'')(i+1)}, r)}} \\ dis(x_{(i)(i+1)}, r) = dis(x_{(i)(i')}, r) + dis(x_{(i')(i'')}, r) + dis(x_{(i'')(i+1)}, r) \\ dis(x_{(N)(1)}, r) = dis(x_{(N)(N')}, r) + dis(x_{(N')(N'')}, r) + dis(x_{(N'')(1)}, r) \\ \phi(x_{(i)(i+1)}, r) \equiv (\phi(x_{(i)(i')}, r), \phi(x_{(i')(i'')}, r), \phi(x_{(i'')(i+1)}, r)) \\ \text{along with, } \tau_1 = 0; i = 1, 2, \dots, N; r \in \{1, 2, \dots, R\}$$

$$\text{Also, } \lambda = \xi / (\kappa \psi), s = \tau + g \sin \phi(x_{(i)(i+1)}, r) + g c_r \cos \phi(x_{(i)(i+1)}, r), \\ \gamma = 1/(1000 \omega e), y = K_e N_e V_e \text{ and } \beta = 0.5 c_d \rho a.$$

**Table 2**

Notations and descriptions of parameters and decision variables.

Notations	Description
N	total number of nodes/retailers
$i, j$	index set for nodes, $i=1$ is the depot
$r$	index of routes $r \in \{1, 2, 3, \dots, R\}$ , R is the maximum number of routes
$x_i$	$i$ th visiting node
$dis(x_{(i)(i+1)}, r)$	distance between $i$ th to $(i+1)$ th node in $r$ th route
$dis^L(x_{(i)(i+1)}, r)$	landslide prone distance between $i$ th to $(i+1)$ th node in $r$ th route
$v(x_{(i)(i+1)}, r)$	vehicle velocity between $i$ th to $(i+1)$ th node in $r$ th route
$c(x_{(i)(i+1)}, r)$	fixed carrying cost from $i$ th to $(i+1)$ th node (without goods) in $r$ th route per unit distance
$c^f(x_{(i)(i+1)}, r)$	fixed charge cost for travel from $i$ th node to $(i+1)$ th node along $r$ th route
$t^f(x_{(i)(i+1)}, r)$	fixed (toll plaza) time taken for travel from $i$ th node to $(i+1)$ th node along $r$ th route
$\phi(x_{(i)(i+1)}, r)$	angle of the road from $i$ th node to $(i+1)$ th node with the horizon along $r$ th route
$P(x_{(i)(i+1)}, r)$	probability of landslide occurrence from $i$ th node to $(i+1)$ th node in $r$ th route
$D^L(x_{(i)(i+1)}, r)$	amount of debris from $i$ th node to $(i+1)$ th node along $r$ th route
$T^q(x_{(i)(i+1)}, r)$	torque of landslide area from $i$ th node to $(i+1)$ th node along $r$ th route
$t^L(x_{(i)(i+1)}, r)$	total landslide recovery time from $i$ th node to $(i+1)$ th node in $r$ th route
$\lambda^{uc}$	unloading cost per unit goods weight
$p_h$	penalty cost per unit time deviation (before time), $h=1, 2, 3$ ( $p_1 < p_2 < p_3$ )
$p'_h$	penalty cost per unit time deviation (after time), $h=1, 2, 3$ ( $p'_1 < p'_2 < p'_3$ )
$U(i)$	$i$ th retailer's dissatisfaction
$\sigma$	carrying cost per unit distance per unit goods weight
$t'$	amount of debris per unit torque per unit distance
$t''$	per unit debris recovery time by the available rescue team
$[a''', b''']$	acceptable time window of the $i$ th retailer for receiving goods
$\tau_i$	unloading time per unit amount of goods at $i$ th node
$-i[a] - j[.] -$	travel from $i$ th node to $j$ th node through the $a$ th route
NSGA-II	Non-dominated sorting genetic algorithm II
MOEA/D	Multi-objective evolutionary algorithm based on Decomposition
mMOTLBO	Modified Multi-objective teaching learning based optimization
$NFS$	no feasible solution
$TCE$	total carbon emission
$\mu$	curb weight (kg)
$t_i$	time for entry in $i$ th node
$d_i$	demand at $i$ th node
$\pi(i)$	total penalty cost at $i$ th node
$[a_i, b_i]$	operation time of the $i$ th retailer
<b>Vehicle independent parameters</b>	
$\xi$	Fuel-to-air mass ratio
$g$	Gravitational constant ( $m/sec^2$ )
$\rho$	Air density ( $kg/m^3$ )
$\tau$	Acceleration ( $m/sec^2$ )
$c_r$	Coefficient of rolling resistance
$\omega$	Efficiency parameters for diesel engines
$\kappa$	Heating value of a typical diesel fuel (kJ/g)
$\psi$	Conversion factor (g/l)
<b>Vehicle dependent parameters</b>	
$K_e$	Engine friction factor (kJ/rev/l)
$N_e$	Engine speed (rev/sec)
$V_e$	Engine displacement (l)
$F_a$	Frontal surface area ( $m^2$ )
$c_d$	Coefficient of aerodynamic drag
$\epsilon$	Vehicle drive train efficiency
$U$	Conversion factor

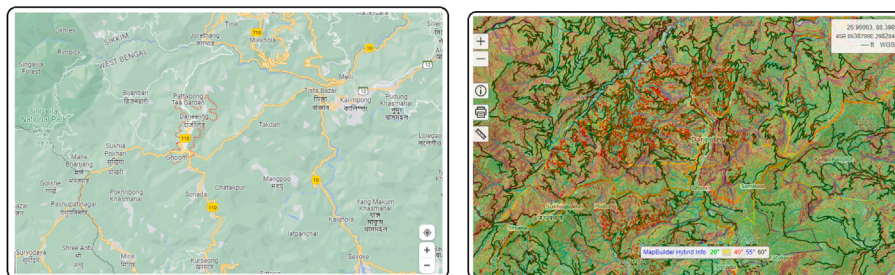
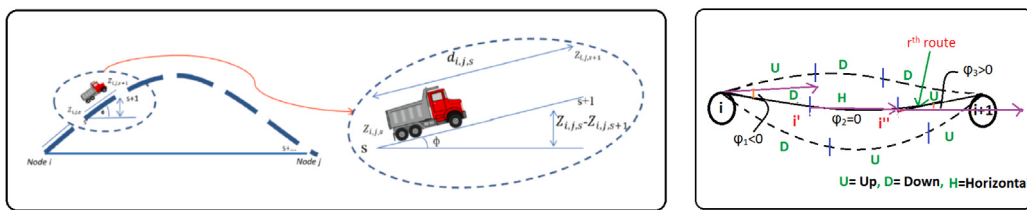


Fig. 2. Google Map with slope of Darjeeling.

The above calculation to determine  $\lambda, \gamma, y$ , and  $\beta$  are based on various parameters of the vehicle, which are fixed for a particular vehicle within the same circumference. The value of  $s$  is based on the road gradient of the paths in the hilly regions. The details of all these parameters are shown in Table 2 and corresponding values are presented in Table 7.

### 3.3.3. Estimation of landslide and its recovery time

**Probability of landslide occurrence** [22]. Logistic regression (LR) is selected as the most suitable technique for predicting the occurrence of landslides based on the underlying factors that contribute to their likelihood [48]. Landslide susceptibility study frequently makes use of LR models [49]. Eq. (3) is a description of the generic linear equation



(a) Road gradient measurement

(b) Slope wise different measurement

Fig. 3. Road gradient measurement.

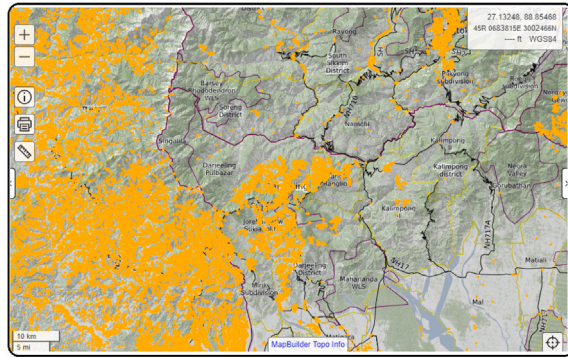


Fig. 4. Landslide prediction in Darjeeling.

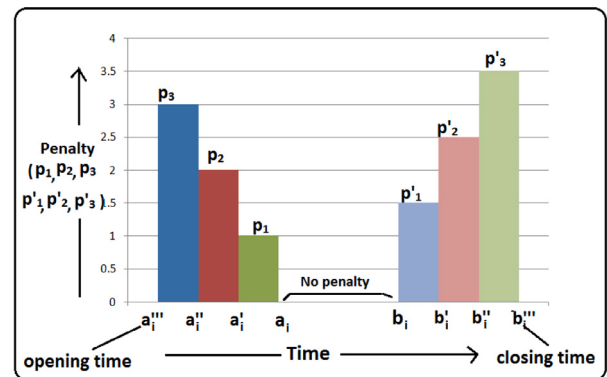


Fig. 5. Satisfaction on time window.

that follows:

$$L = \beta_0 + \beta_1 X_1 + \beta_2 X_2 + \cdots + \beta_n X_n \quad (3)$$

where,  $L$  ( $-\infty$  to  $+\infty$ ): the linear combination  $\beta_i$ 's ( $i = 1, 2, 3, \dots$ ), the coefficients of landslide predisposing factors,  $\beta_0$ : the constant of the equation,  $X_i$ : the predisposing factors (in this investigation,  $i = 1, 2, 3, 4$ ). Here, these factors are the torque of that prone area, the gradient of the road, weather conditions during routing time, and the nature of the soil.

The LR model uses the following Eq. (4), a link function, to predict the probability whether landslides will occur or not in a given location [50]:

$$P(x_{(i)(i+1)}, r) = \frac{1}{1+\exp^{-L}} \quad (4)$$

where  $P(x_{(i)(i+1)}, r) \in [0, 1]$  is the probability of landslide occurrence between  $i$ th to  $(i+1)$ th node using  $r$ th route. The probability of a landslip occurring is calculated using this link function and Eq. (3).

**Amount of landslide-debris.** If the torque of a particular landslide-prone area (cf. Figs. 1 and 4) is  $T^q(x_{(i)(i+1)}, r)$ , spreading through the distance  $dis^L(x_{(i)(i+1)}, r)$  km (say), and  $l'$  is the amount of debris per unit torque per unit distance (known from the past data), then the total amount of debris ( $D^L(x_{(i)(i+1)}, r)$ ) through landslide is calculated using Eq. (5).

$$D^L(x_{(i)(i+1)}, r) = T^q(x_{(i)(i+1)}, r) * dis^L(x_{(i)(i+1)}, r) * l' \quad (5)$$

**Landslide debris recovery time.** In this inquiry, for the sake of simplicity, we take landslip recovery time for a specific path as

$$\begin{aligned} t^L(x_{(i)(i+1)}, r) &= P(x_{(i)(i+1)}, r) * T^q(x_{(i)(i+1)}, r) * dis^L(x_{(i)(i+1)}, r) * l' * t' \\ &= P(x_{(i)(i+1)}, r) * D^L(x_{(i)(i+1)}, r) * t' \end{aligned} \quad (6)$$

where  $t'$  is the per unit debris recovery time by the available rescue team.

### 3.3.4. Customers' (retailers') satisfaction and dissatisfaction

The primary reason for retailer's dissatisfaction is that deliveries of ordered goods are not on time. In this part, we describe the details of retailer dissatisfaction.

**Customer's Dissatisfaction due to delivery outside the Time Window:** Delivery plans prioritize consumer-specified time windows for efficient routing and timely deliveries. Retailers are fully satisfied if the delivery is made within time windows, deviation from that leads to a reduced satisfaction level and the imposition of penalty costs to the supplier. The total dissatisfaction ( $U(i)$ ) for an entire path is calculated through Eq. (7). From Fig. 5 for a particular  $i$ th node, opening and closing times of the shop are  $a_i'''$  and  $b_i'''$  respectively. But, the acceptable time window where dissatisfaction is zero is  $[a_i, b_i]$ . The penalty is incurred when the delivery takes place outside the acceptable time window. The cumulative time, denoted as  $t_{i+1}$ , is calculated when the goods vehicle reaches the  $(i+1)$ th node.

For  $i$ th retailer, the dissatisfaction  $U(i)$  is given by

$$U(i) = \begin{cases} \frac{(a_i - t_i)}{(a_i - a_i''')} & : a_i''' \leq t_i < a_i \\ 0 & : a_i \leq t_i \leq b_i \\ \frac{(t_i - b_i)}{(b_i''' - b_i)} & : b_i < t_i \leq b_i''' \end{cases} \quad (7)$$

where  $t_i$  is the actual delivery time for the  $i$ th retailer.

$$\begin{aligned} t_i &= t_{i-1} + \underbrace{(d_{i-1} * \tau)}_{\text{Unloading Time}} + \underbrace{\left(\frac{dis(x_{(i-1)(i)}, r)}{v_{(x_{(i-1)(i)}, r)}}\right)}_{\text{Traveling Time}} + \underbrace{t^f(x_{(i-1)(i)}, r)}_{\text{Fixed Time}} \\ &+ \underbrace{t^L(x_{(i-1)(i)}, r)}_{\text{Land Sliding recover time}}, \text{ where, } i = 2, 3, \dots, N \end{aligned} \quad (8)$$

### 3.3.5. Formulation of SMO3DDPwCS models

The mathematical formulation of the proposed model is presented (follows the description of 3D multi-objective TSP [51]) as follows:

**Model A: Carbon emission and customer dissatisfaction minimization**

The objective of this proposed SMO3DDPwCS model is to minimize both carbon emissions and customer dissatisfaction (cf. Eq. (9)).

$$\text{Min } CE \text{ and } \text{Min } \sum_{i=2}^N U(i) \quad (9)$$

**Corresponding cost and time:** Management may want to know the cost incurred and time required in this process, which is given by the following Eqs. (10) and (16) respectively.

$$\begin{aligned} \text{Total cost} = Z = & \underbrace{F}_{\text{Fuel Cost}} + \underbrace{\sum_{i=1}^{N-1} c(x_{(i)(i+1)}, r) * dis(x_{(i)(i+1)}, r) + c(x_{(N)(1)}, r) * dis(x_{(N)(1)}, r)}_{\text{Road dependent fixed carrying Cost}} \\ & + \underbrace{\sum_{i=2}^{N-1} \sigma * [D - \sum_{j=2}^i (d_j)] * dis(x_{(i)(i+1)}, r)}_{\text{Goods carrying Cost}} + \underbrace{\sum_{i=1}^{N-1} c^f(x_{(i)(i+1)}, r) + c^f(x_{(N)(1)}, r)}_{\text{Fixed Cost}} \\ & + \underbrace{\sum_{i=2}^{N-1} (d_i * \lambda^{UC})}_{\text{Unloading Cost}} + \underbrace{\sum_{i=2}^N \pi(i)}_{\text{Penalty Cost}} \end{aligned} \quad (10)$$

$$\begin{aligned} \text{where } F = & \sum_{i=1}^{N-1} L\lambda \left[ y \left( \frac{dis(x_{(i)(i+1)}, r)}{v_{(x_{(i)(i+1)}, r)}} \right) + \gamma \beta dis(x_{(i)(i+1)}, r) v^2(x_{(i)(i+1)}, r) \right. \\ & + \gamma s \{ \mu + (D - \sum_{t=2}^i d_t) \} dis(x_{(i)(i+1)}, r) \\ & \left. + L\lambda \left[ y \left( \frac{dis(x_{(N)(1)}, r)}{v_{(x_{(N)(1)}, r)}} \right) + \gamma \beta dis(x_{(N)(1)}, r) v^2(x_{(N)(1)}, r) + (\gamma s \mu) dis(x_{(N)(1)}, r) \right] \right] \end{aligned} \quad (11)$$

$$\text{subject to } D = \sum_{j=1}^N d_j \text{ and } d_i = 0 \quad (12)$$

The penalty cost is incurred when the delivery takes place outside the acceptable time window (cf. Fig. 5), which is calculated as

$$\pi(i) = \begin{cases} (a_i - t_i) * p_1 & : a'_i \leq t_i < a_i \\ (a_i - t_i) * p_2 & : a''_i \leq t_i < a'_i \\ (a_i - t_i) * p_3 & : a'''_i \leq t_i < a''_i \\ 0 & : a_i \leq t_i \leq b_i \\ (t_i - b_i) * p_1' & : b_i < t_i \leq b'_i \\ (t_i - b_i) * p_2' & : b'_i < t_i \leq b''_i \\ (t_i - b_i) * p_3' & : b''_i < t_i \leq b'''_i \end{cases} \quad (13)$$

$$p'_i > p_i, \quad p_i < p_{i+1}, \quad \text{and} \quad p'_i < p'_{i+1}; \quad \forall i \quad (14)$$

Additionally, the goods transportation cost is dependent on the weight of the transported materials, leading to a gradual decrease in weight as the supplier continues visiting the nodes. In this context, we introduce the concept of Discontinuous Goods Transportation Cost, presented as All Unit Discount (AUD), which is defined as follows.

$$\sigma = \begin{cases} \sigma_1 & : 0 < W \leq w_1 \\ \sigma_2 & : w_1 < W \leq w_2 \\ \sigma_3 & : w_2 < W \leq w_3 \\ \sigma_4 & : w_3 < W \leq \infty \end{cases} \quad (15)$$

Here,  $\sigma$  denotes the goods transportation charges per unit weight per unit distance. Where,  $\sigma_1 > \sigma_2 > \sigma_3 > \sigma_4$  and  $w_1 < w_2 < w_3 < w_4$  and  $W$  is the weight of the goods carried by the vehicle.

Total time spent by the system is evaluated using Eq. (16).

$$\begin{aligned} T = & \underbrace{\sum_{i=1}^{N-1} \left( \frac{dis(x_{(i)(i+1)}, r)}{v_{(x_{(i)(i+1)}, r)}} \right) + \left( \frac{dis(x_{(N)(1)}, r)}{v_{(x_{(N)(1)}, r)}} \right)}_{\text{Traveling Time}} + \underbrace{\sum_{i=1}^{N-1} t^f(x_{(i)(i+1)}, r) + t^f(x_{(N)(1)}, r)}_{\text{Fixed Time}} \\ & + \underbrace{\sum_{i=2}^{N-1} (d_i * \tau)}_{\text{Unloading Time}} + \underbrace{\sum_{i=1}^{N-1} t^L(x_{(i)(i+1)}, r) + t^L(x_{(N)(1)}, r)}_{\text{Landslide recovers time}} \end{aligned} \quad (16)$$

**Model B: Carbon emission and customer dissatisfaction minimization with time constraints**

If the management wants to complete the whole delivery process within a specific time limit,  $T_{max}$ , say then the optimization problem is

$$\text{Model A, subject to, } T \leq T_{max} \quad (17)$$

**Model C: Carbon emission and customer dissatisfaction minimization with cost constraints**

On the other hand, if the management wants to put an upper limit on the total cost incurred during the whole process, then the optimization problem is reduced to

$$\text{Model A, subject to, } Z \leq Z_{max} \quad (18)$$

**Model D: Carbon emission and customer dissatisfaction minimization with both (time and cost) constraints** If the upper limits on both total time and cost for the whole process, are imposed by the management, then the problem is reduced to

$$\text{Model A, subject to, } T \leq T_{max} \text{ and } Z \leq Z_{max} \quad (19)$$

#### 4. Proposed modified multi-objective teaching learning based optimization algorithm (mMOTLBO)

Here, we develop the modified teaching learning based optimization (mMOTLBO) to solve multi-objective problems. In this mMOTLBO approach, we maintain an external archive to store the best solutions obtained during the optimization process. We incorporate the non-dominated sorting concept from NSGA-II [52] to select the individuals from better fronts, thus guiding the population towards the Pareto front (PF). Furthermore, we utilize the crowding distance computation mechanism employed in NSGA-II [52] to preserve diversity among the current best solutions stored in the external archive. Detailed explanations of these methods are provided in the subsequent sections.

TLBO imitates the learning dynamics between a teacher and a population of learners. Within TLBO, multiple learners collectively form a population of activities. The best-performing learner from the current population is chosen as the teacher. Each learner undergoes two distinct phases: teaching phase and learning phase (cf. Fig. 6).

In this study, we introduce modifications to both teaching and learning phases, along with the self-learning concept to develop modified TLBO (mTLBO). In the teaching phase, we implement a new upgradation strategy to enhance the learning process. Meanwhile, in the learning phase, we adopt an interactive group-based crossover approach to further improve the learners' performance. Two different self-learning approaches are introduced after the teaching and learning phase. These modifications aim to enhance the overall effectiveness and efficiency of the TLBO algorithm.

##### 4.1. Representation

Fig. 7 illustrates an example of an arbitrary learner represented as a one-dimensional vector. Let this learner traverse through 5 different subjects or nodes while adhering to the conditions of the TSP.

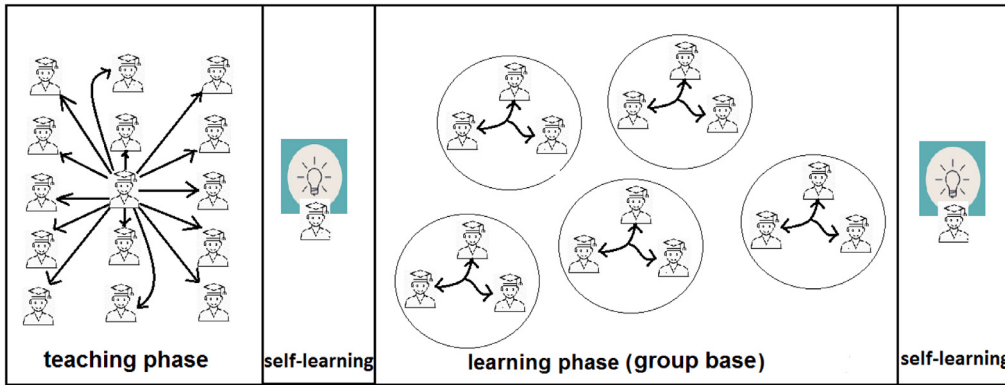


Fig. 6. Schematic diagram of TLBO.

learner	1[2]	2[1]	4[0]	5[2]	3[1]	1
---------	------	------	------	------	------	---

Fig. 7. Learner (path with 5 nodes).

learner 1	1[2]	2[1]	4[0]	5[2]	3[1]	1
learner 2	1[0]	3[2]	5[1]	2[2]	4[0]	1
learner 3	1[2]	5[1]	2[2]	4[0]	3[2]	1
learner 4	1[1]	4[0]	3[2]	2[1]	5[0]	1

Fig. 8. Initialization with 4 learners (5 nodes each).

#### 4.2. Initialization

To construct  $M$  routing paths for  $N$  nodes, we create a total of  $M$  learners, where  $N$  represents the different subjects (nodes) and  $M$  represents the population size. Each routing path represents a different learner. These paths are randomly generated while adhering to the Traveling Salesman Problem (TSP) conditions. Let us assume that  $f(x_i)$  denotes the fitness function of the  $i$ th learner, where  $i$  ranges from 1 to  $M$ . An example of 4 learners with 5 nodes is depicted in Fig. 8. Each learner represents a different routing path that satisfies the TSP constraints.

#### 4.3. Boltzmann selection

Initially, we calculate the Boltzmann probability [53] for each learner in the initial population using

$$p_B = e^{(g/G)*(f_{min} - f(x_i))/KT},$$

where:  $p_B$  is the probability of each learner.  $T = T_0(1 - a)^k$ , where  $k = (1 + C \cdot \text{rand}[0, 1])$ , and  $C = \text{rand}[1, 100]$ .  $g$  represents the current generation number, and  $G$  is the maximum generation.  $T_0$  and  $a$  are random values in the range [50, 140] and [0, 1] respectively.  $f(x_i)$  is the objective function of the learner.  $f_{min}$  is the minimum value of the objective function among all learners.  $i = 1, 2, \dots, M$ , where  $M$  is the total number of learners in the population. Next, we assign a predefined value, say the probability of selection ( $p_s$ ). For each learner with objective function value  $f(x_i)$ , we generate a random number,  $r \in [0, 1]$ . If  $r < p_s$  or  $r < p_B$ , then the corresponding learner is selected for the teaching phase. Otherwise, the learner associated with  $f_{min}$  is chosen for the teaching phase.

#### 4.4. Upgraded teaching phase with self-learning

##### 4.4.1. Upgraded teaching phase

In mMOTLBO, we introduce an upgradation strategy in the teaching phase, as depicted in Fig. 9. The algorithm for this teaching phase is presented in Algorithm 1.

##### Algorithm 1: UPGRADED TEACHING PHASE

```

1 randomly generate M learner
2 evaluate all fitness of the learner
3 teacher=best learner (based on fitness)
4 for i ← 1 to M do
5   diff(i)=(T-f(xij)) for j ← 1 to N do
6     new xij=1+(rand(1,diff(i))+xij)%N
7     update xij maintaining TSP condition satisfied
8   if f(new xij) better than f(xij) then
9     xij=new xij
10  else
11    xij=xij

```

##### 4.4.2. Self-learning after teaching phase

This self-learning initiative is by the teacher. The following process (Fig. 10) shows how self-learning strategies perform based on the teacher's influence.

#### 4.5. Interactive group-based learning with self-learning

##### 4.5.1. Interactive group based learning

The learning phase incorporates a group-based learning strategy, inspired by real-life scenarios among learners. This learning strategy utilizes an interactive crossover (shown in Fig. 11). The learners form groups and randomly interact with one another, facilitating mutual enrichment. For this investigation, we form groups with an equal number of learners. Within these groups, all learners engage in competition and interaction with each other to upgrade themselves (refer to Algorithm 2). This process allows learners to learn from each other and improve their performance collectively.

In this scenario, let us consider a group with an equal number of learners ( $K = 3$ , for example) as shown in Fig. 6. To upgrade individual learners within the group, we illustrate an example of a five-node TSP, which is depicted in Fig. 11.

##### 4.5.2. Self-learning after learning phase

This is a self-learning initiative by the learner/peer group. Through the peer group, the learner may enrich their learning capacity or be diverted from the topic. The generation-dependent odd mutation-based

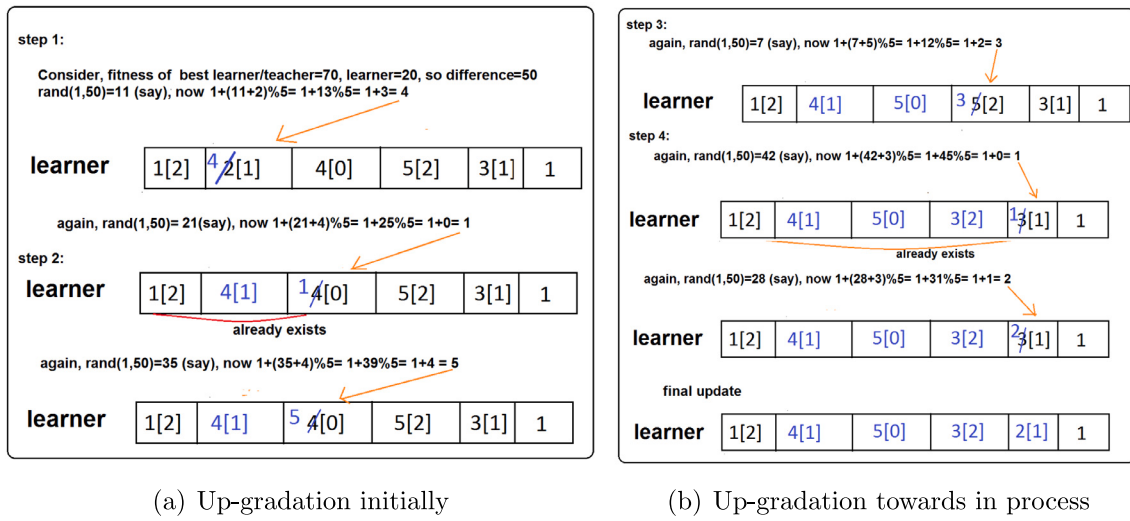


Fig. 9. Up-gradation strategy of learner.

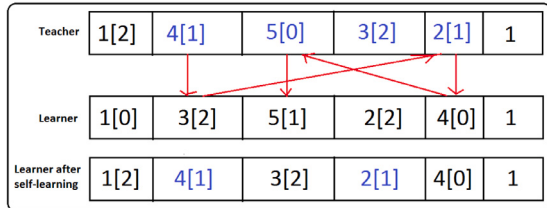


Fig. 10. Self-learning process.

**Algorithm 2:** INTERACTIVE GROUP BASED LEARNING

```

1 population size= number of learners (M)
2 total number of distinct groups (TG)=M/K //K=number of
   learner in each group
3 for i ← 1 to TG do
4   choose K distinct learner from the group
5   for t ← 1 to K do
6     for j ← 1 to N do
7       the first node of each learner are same (say si)
8       choose next node (say lnew)= min(si, each next
         unvisited node of the K learners)
9       update learner with lnew node
10      si=lnew

```

concept is introduced to a learner for self-learning. With this concept, premature convergence is avoided. The value of  $p_m$  is evaluated depending on the generation using a specific function.

$$p_m = \frac{k}{\sqrt{\text{odd number corresponding current generation number}}}, k \in [0,1].$$

For odd numbers 1, 3, 5, 7, ...,  $p_m$  is  $\frac{k}{\sqrt{1}}, \frac{k}{\sqrt{3}}, \frac{k}{\sqrt{5}}, \dots$  as generation progress.

If the condition  $r < p_m$ , where  $r \in [0,1]$ , is satisfied, then the corresponding learner is selected for mutation. Subsequently, random mutation (as depicted in Fig. 12) is performed based on the calculated value of  $p_m$ . This dynamic approach ensures that the mutation operation is applied selectively to learners, enhancing the exploration of the solution space and potentially improving the optimization process.

**4.6. External archive**

We integrate an external archive to save the most promising solutions developed in order to improve the performance of the mMOTLBO algorithm. This includes non-dominated sorting and crowding distance computation into the algorithm, particularly in the selection of Teachers and the population deletion mechanism. As a result, we create an external archive that houses the most recent and best solutions.

**4.7. Selection operator**

We select the teacher for the learners from the non-dominated solutions with the largest crowding distance values. This strategy allows the learners in the primary population to gravitate towards non-dominated solutions in the external archive located in less crowded areas within the objective space. We choose different teachers for each learner in a specified top portion of the external archive, prioritizing solutions with decreasing crowding distance values. Furthermore, we select the centroid of non-dominated solutions from the current archive as the mean for the learners, which contributes to the learners' overall performance during the optimization process. If the candidate outperforms the teacher or peer group, the teacher is replaced. If the teacher outnumbers the learner, the learner is eliminated. When both learner and teacher are non-dominated with regard to each other, we choose one at random to join the population.

**4.8. Non-dominated sorting**

According to the method proposed by Deb et al. [52], each solution in the population needs to be compared to every other solution to determine if it is dominated, allowing the population to be sorted based on the level of non-domination. This method is repeated until all fronts are identified, resulting in the population being divided into multiple fronts based on the degree of non-domination. This process helps in organizing the solutions based on their Pareto optimality and provides a clear understanding of the trade-offs between different objectives in multi-objective optimization problems.

**4.9. Crowding distance sorting**

The crowding distance, proposed by Deb et al. [52], is utilized to approximate the density of solutions in the population surrounding an individual solution  $i$ . This approach for estimating the crowding degree is used in two instances. Firstly, when the goal vector and trial vector do

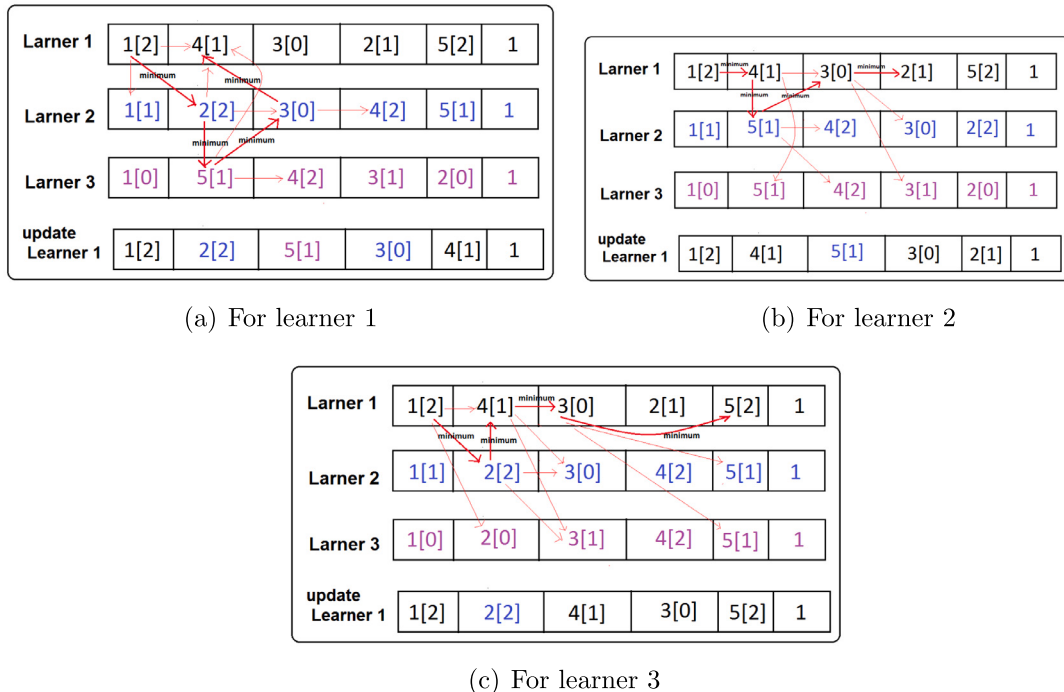


Fig. 11. Interactive group based crossover among three learner.

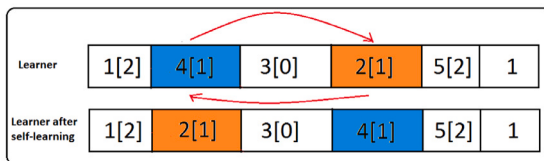


Fig. 12. Self-learning process.

not dominate each other, we evaluate the crowding degree of the target vector and trial vector in comparison to the non-dominated solutions in the external archive. The less crowded solution is selected as the target vector for the next generation. Secondly, when the external archive exceeds a certain size, it becomes necessary to identify and remove solutions located in the most congested regions.

#### 4.10. Avoiding premature convergence in mMOTLBO

The increased search space in multi-objective problems amplifies the risk of premature convergence. To address this, we have incorporated the following mechanisms into the modified Teaching–Learning-Based Optimization (mMOTLBO) algorithm.

In Sections 4.4.1 and 4.4.2, the upgraded teaching phase and self-learning teaching phase, respectively, are employed based on the node size of the benchmark instances. These mechanisms are enhanced for different node sizes of the benchmark instances and are designed to explore the solution space effectively.

In Section 4.5.1, interactive group-based learning is used to promote interaction among learners, leading to better exploitation of promising areas in the search space. In Section 4.5.2, generation-dependent self-learning after the learning phase enables individual learners to improve independently, further reducing the chances of premature convergence. An external archive (Section 4.6) is maintained to store the best solutions identified during the optimization process. Using the non-dominated sorting method from NSGA-II, the solutions are organized into Pareto fronts, progressively guiding the population towards the

true Pareto front (PF). To preserve diversity, the crowding distance mechanism (Section 4.9) from NSGA-II is applied within the external archive. This ensures exploration of diverse regions in the search space and avoids premature convergence to suboptimal solutions.

These strategies collectively enhance the algorithm's ability to balance exploration and exploitation, effectively addressing the challenges posed by the expanded search space in multi-objective optimization.

#### 4.11. Flowchart and algorithm of mMOTLBO

The flowchart of mMOTLBO is presented in Fig. 13.

A combination of the above steps leads to the algorithm of the proposed mMOTLBO (Algorithm 3).

The mMOTLBO algorithm is a combination of various techniques, including Boltzmann selection, a new upgradation strategy in the teaching phase, and a novel interactive group-based crossover for learners in the learning phase, along with self-learning. These techniques work together to improve the optimization process, enhance exploration and exploitation of the solution space, and achieve better convergence towards optimal solutions in multi-objective optimization problems. The algorithm was implemented in C++ with a population size of 100 learners and a maximum of 1000 iterations.

#### 4.12. Performance metric/indicator

The true Pareto optimal front, denoted as  $P_{true}$ , serves as a key metric to evaluate the efficacy of a Multi-Objective Optimization Problem (MOOP) algorithm. This front is commonly employed as a standard reference for comparing the approximate Pareto optimal fronts generated by various methods for a specific problem instance.

In Multi-Objective Optimization Problems (MOOPs) due to the conflicting nature of objectives, different performance measures or indicators are utilized to assess an algorithm's effectiveness [54]. These performance indicators [55] aim to evaluate the fundamental objectives of MOOPs. Firstly, determine how close the resulting Pareto front is to the true Pareto optimal front of the considered MOOP using

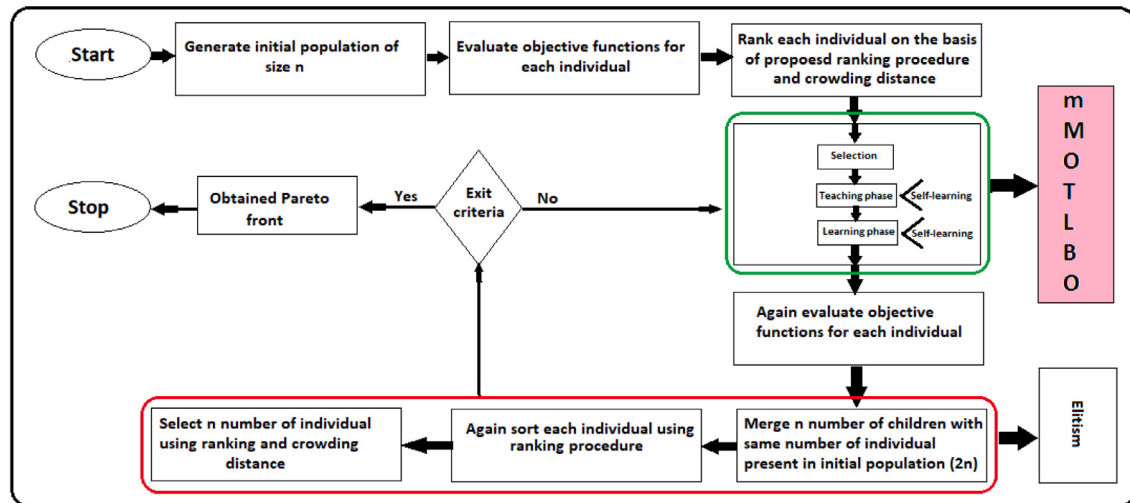


**Fig. 13.** Flowchart of mMOTLBO.

**Algorithm 3:** Algorithm of mMOTLBO

```

Data:  $M$  = population size
Result: Set of non-dominated solutions (Pareto front)

1 popu ← Initial population ( $M$ )
2 Proposed non-dominated rank (popu)
3  $gen \leftarrow 0$ 
4 while  $gen \neq MaxGen$  do // maximum generation
5    $M_x \leftarrow M + 1$  //  $M_x$  is where new learner are
     stored
6   for  $j \neq 2M$  do
7     Teaching phase: perform using Algorithm 1.
8     self-learning phase: perform using sub-section 4.4.2.
9     Learning phase: perform using Algorithm 2
10    self-learning: perform using sub-section 4.5.2.
11    if  $Learner_{old} < Learner_{new}$  then
12       $Learner_{old} \leftarrow Learner_{new}$  // Replace the better
13    else
14      Retain  $Learner_{old}$ 
15   Proposed non-dominated rank (popu) // size of popu
     is  $2M$ 
16   Crowding distance (popu)
17   Select  $M$  number of solution from the popu of size  $2M$ 
18    $gen \leftarrow gen + 1$ 
19 return a set of Pareto front

```

**Table 3**  
 Notations, description and parametric values of all multi-objective algorithms.

Notation	Description
NSGA-II	Roulette Wheel Selection, Cyclic Crossover, Random Mutation
mNSGA-II	Probabilistic Selection, Cyclic Crossover, Generation Dependent Mutation
MOEA/D	Multi-objective Evolutionary Algorithms based on Decomposition
mMOTLBO	Boltzmann Selection, Upgradation Strategy, and Interactive Group-based Crossover
Parameters	Value/Range
Max_Generation	1000
$p_s$	.54
learner/chromosome	100
K(learner in each group)	3

### 5.1. Benchmark problems

A multi-objective TSP instance is created by merging two conventional TSP instances of the same size. There is currently a very limited accepted benchmark set specifically designed for MOTSP in the literature [51,57,59–62]. Most studies have relied on either randomly generated test cases or instances combining single-objective standard problems from TSPLIB [10]. In the present study, we adopted the methodology of creating synthetic multi-objective instances by combining two single-objective standard instances from TSPLIB of identical sizes from number nodes 29 to 200 and ensures that the generated instances are representative and challenging. Seven multi-objective TSP instances with sizes 29, 76, 100, 150, and 200 are taken for the experiment. For the sake of simplicity, bi-objective TSP problems are solely taken into account in this case. These are baysbayg29, eilpr76, kroAB100, kroAC100, kroBC100, kroAB150, and kroAB200 taken from TSPLIB [10] and are given in [https://github.com/somnathmajivucs/MOTLBO\\_input\\_data](https://github.com/somnathmajivucs/MOTLBO_input_data). Table 4 displays the optimal solutions of various TSP cases used to build MOTSP instances. Six Pareto optimal solutions are offered for each instance of MOTSP, two of which contain the optimum values of the objectives of the respective TSPs.

As previously explained, the algorithm to find a Pareto front is executed ten times with different seeds of a random number generator, resulting in ten non-dominated fronts. Combinations of these fronts create a solution set, which may contain solutions that are not non-dominated. To obtain the Pareto front of the problem using the algorithm, we remove all the dominated solutions from this solution set. Fig. 14 displays the union of all non-dominated solution sets and

## 5. Experimental results of MOOPs

To evaluate the performance of the proposed metaheuristic, it was compared to other existing metaheuristics related to the Multi-Objective Traveling Salesman Problem (MOTSP) in the literature. The comparison was conducted on various test instances with different sizes from TSPLIB. The notations, description, and parametric values of all multi-objective algorithms are presented in [Table 3](#).

**Table 4**  
Test results of benchmark instances.

Instance	NON	Optimal value	MO instances	Six POS	CT (minutes)
bays29	29	2020		(2020,1659) (2022,1641) (2030,1628)	
bayg29	29	1610	baysbayg29	(2072,1610) (2074,1626) (2064,1629)	15.6
eil76	76	538		(597,574242) (613,569684) (671,539035)	
pr76	76	108 159	eilpr76	(2257,111376) (2315,112077) (2353,113279)	31.2
kroA100	100	21 282		(21298,28116 ) (21416,26252) (21587,23417)	
kroB100	100	22 141	kroAB100	(21914,22719) (24318,22464) (27312,22210)	42.87
kroA100	100	21 282		(21305,29318) (21422,26621) (21632,23416)	
kroC100	100	20 749	kroAC100	(21813,21135) (22089,20916) (25182,20756)	39.54
kroB100	100	22 141		(22156,29141) (22372,27387) (22617,24146)	
kroC100	100	20 749	kroBC100	(23931,21312) (25616,20867) (28319,20792)	47.38
kroA150	150	26 524		(26571,33221) (26712,31615) (26953,28132)	
kroB150	150	26 130	kroAB150	(27819,26746) (30241,26312) (34818,26146)	64.57
kroA200	200	29 368		(29417,42613) (30812,39397) (31434,34187)	
kroB200	200	29 437	kroAB200	(33542,30218) (36186,29892) (39392,29612)	93.67

NON: Number of nodes, CT: Computational time, POS: Pareto optimal solutions, MO: Multi-objective

the corresponding Pareto front for all test problems as determined by mMOTLBO, NSGA-II, MOEA/D, and mNSGA-II. The Pareto front of mMOTLBO is marked as red. These graphs illustrate that the density of the Pareto front decreases as the size of the problems increases.

### 5.2. Performance analysis of the proposed algorithm wrt several performance indicators

The statistical data corresponding to the performance measures—ONVG, OTNVG, OTNVGR, and ER are shown in Table 5. This table shows that for each of the test examples, the proposed algorithm yields the largest percentage value of OTNVGR. In light of the OTNVGR measure, the proposed algorithm performs better than the other methods that were taken into consideration. These statistics also show that the ER values of the Pareto optimum fronts produced by the suggested algorithm are minimal in every case. Therefore, when compared to other algorithms, mTLBO performs better in terms of ER. The graphical representation of the ER values may also be seen in Fig. 15.

The convergence of the resulting PF to the  $P_{true}$  are two main criteria of the MOOP algorithm. The IGD evaluates a MOOP algorithm's performance with respect to the above criteria. When the IGD indicator value is 0, it means that the obtained PF and  $P_{true}$  are identical, and

the acquired solutions are dispersed throughout the entire  $P_{true}$ . Table 5 shows that, with the exception of kroAB100 (near zero), the IGD values of the suggested algorithm are all zero. It shows that the acquired Pareto front of the suggested technique is dispersed throughout the whole solution space and is extremely similar to the true Pareto front. Another finding from Table 5 indicates that the mNSGA-II algorithm produces the second-best PF, followed by the NSGA-II and MOEA/D algorithms. As a result, it can be said that mMOTLBO has greater efficiency in terms of the IGD indicator than any other algorithm under examination.

The degree of convergence of the Pareto front is assessed using the Generational Distance (GD), a performance indicator related to convergence. GD measures the typical distance between the solutions constituting the obtained Pareto optimal front, denoted as  $Q$ , (say) and the true Pareto optimal front, denoted as  $P_{true}$ , for the corresponding MOOP instance. A lower GD value indicates that the quality of  $Q$  in relation to  $P_{true}$  is very good. Notably, the proposed approach consistently achieves the lowest GD value for each test instance considered in the experiment. A GD value of zero would indicate that the average Euclidean distance between the obtained Pareto front and the true Pareto front is very small. While none of the algorithms yield a GD value of zero, the proposed methodology outperforms all other methods in terms of providing the best Pareto optimal front in comparison to the other algorithms considered in the tests.

Deb et al. [52] proposed the spread metric to measure the diversity of solutions in the Pareto front of any MOOP. The value of the spread metric ranges between 0 and 1. A smaller spread value indicates better diversity. This metric helps evaluate the quality of the Pareto optimal front. Table 5 shows that the proposed algorithm performs better according to the spread metric indicator.

## 6. A real-life experiment for SMO3DDPwCS

Let us consider a routing problem for a supplier delivering an item to 9 retailers in the Darjeeling district, West Bengal, India, which is a hilly region (Fig. 16). Thus there are 10 nodes (1 depot and 9 retailers) and 3 connecting routes among the nodes and between the depot and nodes.

### 6.1. Different models of SMO3DDPwCSs

Let there is a depot at, Siliguri (marked by node “\*”1), and 9 delivery nodes are (2) Lataguri, (3) Sevoke, (4) Fulbari, (5) Darjeeling, (6) Mirik, (7) Bagdogra, (8) Ghoom, (9) Kalimpong, (10) Gorubathan). Thus SMO3DDPwCSs are formulated following the 3DTSP procedure with 10 nodes and 3 alternative routes for travel between every two nodes (cf. Section 3).

### 6.2. Input data

The data for distance (in km), traveling cost per unit distance (INR), fixed carrying cost (INR), fixed charge cost (INR), fixed charge time (minute) and slopes of the roads (degree), landslide recover time (minute) row-wise 1st, 2nd, 3rd, 4th, 5th, 6th and 7th) are given in [https://github.com/somnathmajivucs/MOTLBO\\_input\\_data](https://github.com/somnathmajivucs/MOTLBO_input_data) are presented. Other parameters of the model are given in Tables 6 and 7.

As shops' operating hours vary from 6:00 to 22:00 (say), the optimal time to receive the items (which varies with retailers) is 9:00-16:00 (say). During the rest of the time, items can be received between 6:00 and 9:00 a.m. and 16:00 and 22:00 p.m., with discontentment due to odd timing, non-availability of workers, etc. Dissatisfaction with the receipt of the item before 9:00 and after 16:00 is calculated using Eq. (7). The delivery of the item before 6:00 and after 22:00 is not acceptable. The vehicle with the item starts from the depot at 6:00. Table 8 shows retailers' availability and order receipt time slots.

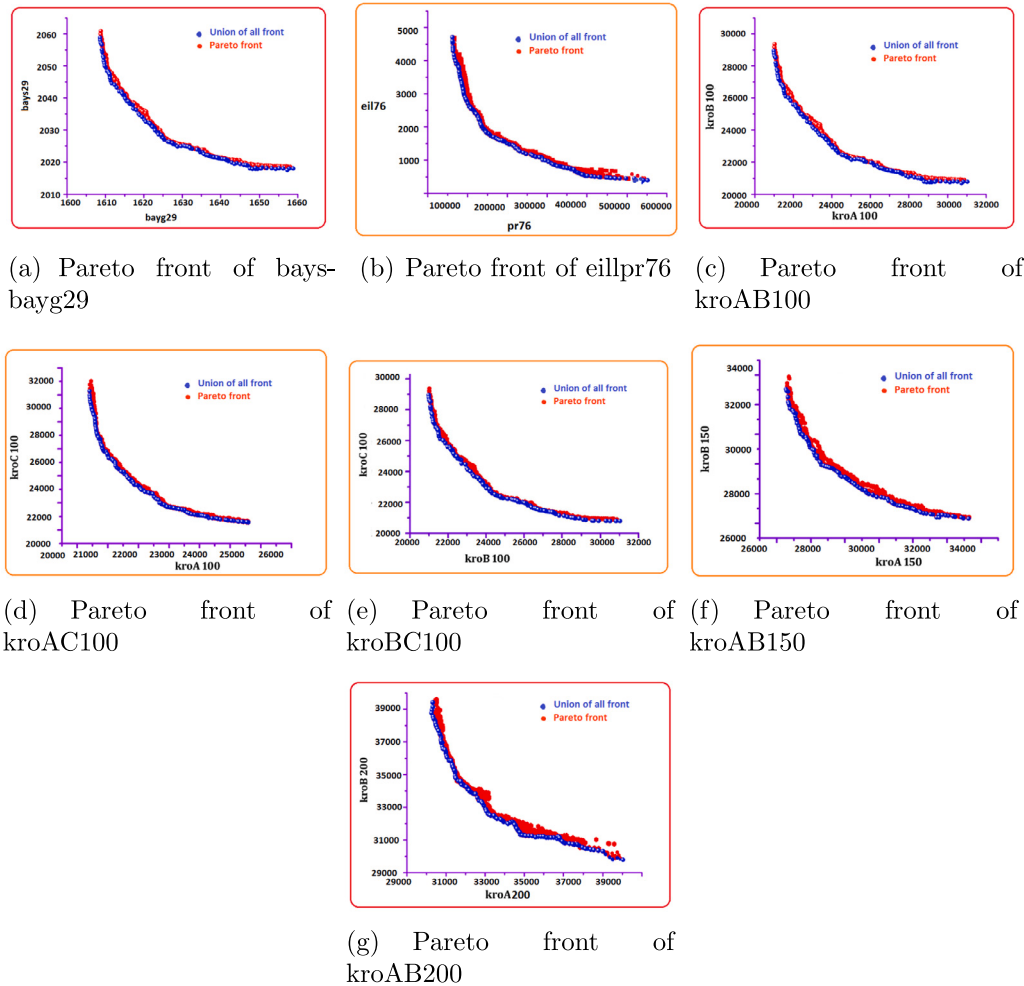


Fig. 14. Pareto front of standard TSP instances.

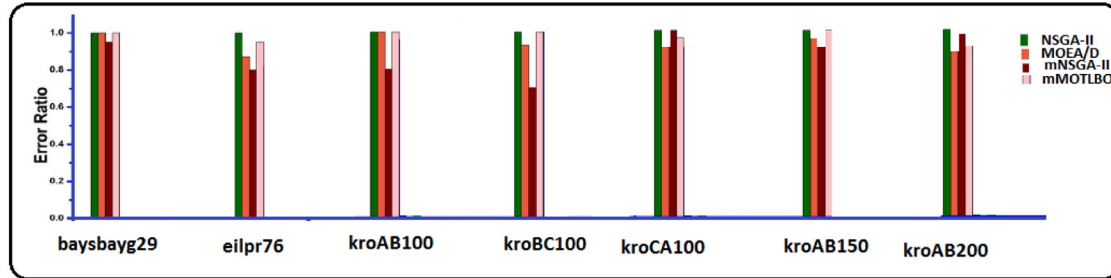


Fig. 15. Error ratios for various algorithms in relation to various instances.

With the above data, we solve the Models-A (Eq. (9)), -B (Eq. (17)), -C (Eq. (18)), -D (Eq. (19)), using the developed mMOTLBO.

### 6.3. Experimental results

#### 6.3.1. Results of Model A (carbon emission and customer dissatisfaction minimization)

Table 9 furnishes the optimum results of TCE, TCDS, total cost and time, and the routing plan (along with paths) of Model A. Here total distance, total cost (fuel, fixed, carrying, goods charge, fixed, unloading, penalty), and total time (travel, fixed, unloading, landslide recover) are presented. From Table 9, for Model A, one of the optimal routing path (OS=1) is  $1[0]^{33.78} 3[1]^{28.28} 2[2]^{26.74} 10[2]^{21.37} 9[1]^{32.59} 5[2]$

$^{27.38} 6[2]^{21.29} 8[2]^{31.37} 7[1]^{25.27} 4[0]^{33.78} 1$ . It means that the delivery vehicle starts from node 1 (depot), moves to node 3rd with velocity 33.78 km/h using 1st path, then moves to node 2nd with velocity 28.28 km/h using 2nd path, after that move to node 10th with velocity 26.74 km/h through 3rd path and so on. Here, the numbers 0, 1, and 2 within [ ] represent the different routes between the two nodes. Total carbon emissions (TCE) and total customer's dissatisfaction (TCDS) are 67.34 kg and 1.10 respectively. The different parametric values are: total routing distance (124 km), total cost (INR 72520.82), total system time (12.11 h.), fuel cost (INR 10315.14), fixed carrying charge (INR 14800), goods charge (INR 40973.68), fixed cost (INR 416), unloading cost (INR 4000), penalty cost (INR 2016), traveling time (5.98 h.),

**Table 5**  
Performance analysis wrt some performance indicators.

Instace	NDSTPF	Different Algo.	ONVG	OTNVG	OTNVGR (%)	DSTPF	ER	IGD	GD	Spread
baysbayg29	84	NSGA-II	52	35	67.30	17	0.32	779.34	104.76	0.94
		MOEA/D	69	39	56.52	30	0.43	612.78	92.79	0.92
		mNSGA-II	63	46	73.01	17	0.26	316.46	84.16	0.91
		mTLBO	82	76	92.68	6	0.07	0.11	4.12	0.89
eilpr76	70	NSGA-II	41	15	36.58	26	0.63	882.31	193.16	0.79
		MOEA/D	52	21	40.38	31	0.59	537.66	184.38	0.81
		mNSGA-II	56	26	46.42	30	0.53	312.36	103.71	0.77
		mTLBO	67	63	94.02	4	0.05	0.19	5.07	0.76
kroAB100	78	NSGA-II	38	29	76.31	9	0.23	716.92	432.36	0.88
		MOEA/D	45	37	82.22	8	0.17	535.32	401.88	0.85
		mNSGA-II	43	36	83.72	7	0.16	189.46	382.76	0.84
		mTLBO	74	69	93.24	5	0.06	0.17	3.95	0.82
kroBC100	65	NSGA-II	40	33	82.50	7	0.17	814.32	235.64	0.91
		MOEA/D	46	35	76.08	11	0.23	582.19	187.32	0.88
		mNSGA-II	47	36	76.59	11	0.23	212.42	120.45	0.87
		mTLBO	62	57	91.93	5	0.08	0.14	10.07	0.85
kroCA100	83	NSGA-II	47	41	87.23	6	0.12	946.18	392.23	0.71
		MOEA/D	58	52	89.65	6	0.10	722.33	361.54	0.72
		mNSGA-II	63	54	85.71	9	0.14	287.68	236.18	0.69
		mTLBO	79	75	94.93	4	0.05	0.13	8.07	0.68
kroAB150	76	NSGA-II	51	40	78.43	11	0.21	1135.14	837.14	0.87
		MOEA/D	62	47	75.80	15	0.24	983.19	742.38	0.88
		mNSGA-II	63	52	82.53	11	0.17	432.76	587.11	0.84
		mTLBO	72	69	95.83	3	0.04	0.11	6.01	0.81
kroAB200	68	NSGA-II	32	22	68.75	10	0.31	1731.32	935.34	0.77
		MOEA/D	38	30	78.94	8	0.21	1247.88	746.52	0.76
		mNSGA-II	42	34	80.95	8	0.19	737.16	322.87	0.74
		mTLBO	63	60	95.23	3	0.04	0.23	12.34	0.71

NDSTPF: Non-dominated solutions in true Pareto front, DSTPF: Dominated solutions in true Pareto front.

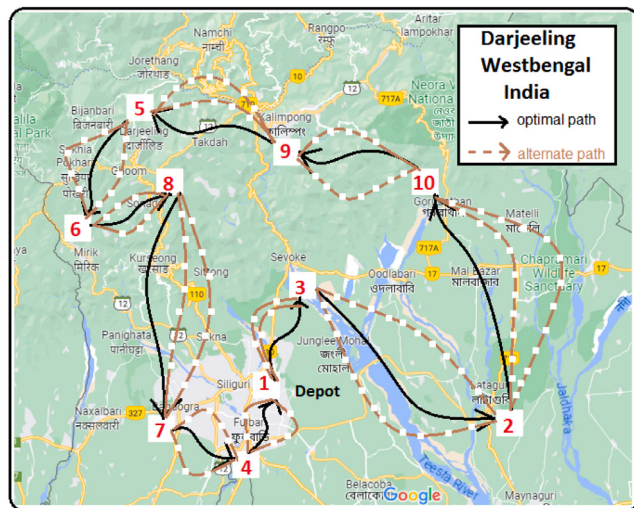


Fig. 16. Optimal path in Darjeeling.

**Table 6**  
Goods delivery matrix.

Node	Material delivery amount, time, cost										
	1	2	3	4	5	6	7	8	9	10	Total
Amount (kg)	0	150	200	220	160	190	250	300	260	270	2000
Unloading time (minute)	0	15	20	22	16	19	25	30	26	27	200
Unloading cost (INR)	0	300	400	440	320	380	500	600	520	540	4000

fixed time (0.11 h.), unloading time (3.33 h.), landslide recover time (2.69 h.).

### 6.3.2. Necessity of modeling with multipaths between nodes

The incorporation of multipath routing in a model is more practical (cf. Fig. 17(a)) and reflective of real-world scenarios, considering the widespread infrastructural development globally, even in developing countries like India, etc. In this study, for the first time, we have considered the existence of three different connecting paths between any two arbitrary nodes. In contrast to having three routes, if there is only a single route (say, route denoted by 0), the optimal results of Model A are evaluated and presented in Table 10. Comparing the results, it is evident that the multipath model performs better. This is also evident from the Pareto front solutions of Model with both multi- and single path depicted in Fig. 17(b).

### 6.4. Segmentwise vs average road slopes

It is observed that the segment-wise slope (cf. Table 9) (which is taken from past records) is more effective than the average road slope (say, 6°) in terms of optimum results shown in Fig. 18.

### 6.4.1. Supremacy of mMOTLBO

If Model A is solved through NSGA-II, mMOTLBO, and MOEA/D, then the Pareto fronts for these methods are obtained and presented in Figs. 17(b) and 19. It is observed from Fig. 19, that the Pareto front by mMOTLBO is better than the other two methods.

### 6.4.2. Ranking of the Pareto fronts of Model-A using the TOPSIS approach

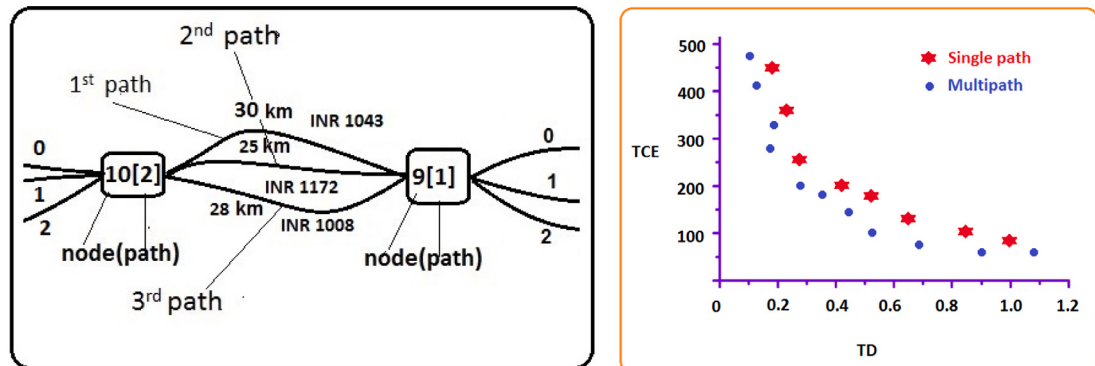
Due to its user-friendliness, TOPSIS is frequently preferred by decision-makers when comparing the scores of many alternatives in the presence of competing criteria [63]. The basic idea behind this method is to determine how close each alternative is to the perfect answer by taking into account both the distance from the ideal solution and the unfavorable ideal solution. The Euclidean distance notion is used to carry out this evaluation. Using the normalized decision matrix, weighted normalized decision matrix, positive and negative ideal solution, separation measure, and relative closeness (cf. [64]), we do the ranking of the Pareto front solutions as given in Table 11.

**Table 7**  
Input parameters for the proposed models.

Notation	Values	Notation	Values	Notation	Values	Notation	Values
$\Omega^1$	0.002	$S^2$	0.8929	$L$	1.3730	$\psi$	737
$\Omega^2$	0.0022	$P^1$	0.5083	$t^{im^1}$	40	$g$	9.81
$t^1$	0.00139	$P^2$	0.3846	$t^{im^2}$	50	$\kappa$	44
$t^2$	0.00111	$D_s$	2.7476	$t^e$	0.25	$\phi$	0
$a^1$	0.01373	$F_d$	7.0	$c_d$	0.6	$\omega$	0.45
$a^2$	0.01511	$V_c$	4000	$c_r$	0.01	$\tau$	0
$\theta_1$	15	$N_e$	38.3	$\mu$	3500	$\rho$	1.2041
$\theta_2$	35	$K_e$	0.258	$\varepsilon$	0.45		
$S^1$	0.9616	$V_e$	4.50	$\xi$	1		
$p_1$	1	$p_2$	2	$p_3$	5		
$p'_1$	2	$p'_2$	5	$p'_3$	10		
$w_1$	2000 kg	$w_2$	1500 kg	$w_3$	1000 kg	$w_4$	500 kg
$\sigma_1$	0.010	$\sigma_2$	0.015	$\sigma_3$	0.020	$\sigma_4$	0.030
Velocity	15-35 km/h						

**Table 8**  
Retailers availability matrix.

Time: 24 h format										
Node	1	2	3	4	5	6	7	8	9	10
Opening time	6:00	6:00	10:00	7:00	8:00	7:00	14:00	12:00	9:00	6:00
Satisfied time	6:00-22:00	9:00-12:00	12:00-14:00	8:00-11:00	9:00-12:00	10:00-14:00	15:00-20:00	14:00-18:00	12:00-16:00	7:00-11:00
Closing time	22:00	14:00	16:00	14:00	15:00	17:00	22:00	20:00	18:00	16:00



(a) Justification of multipath

(b) Pareto front for single and multipath

Fig. 17. Pareto front for single and multipath and proposed model.

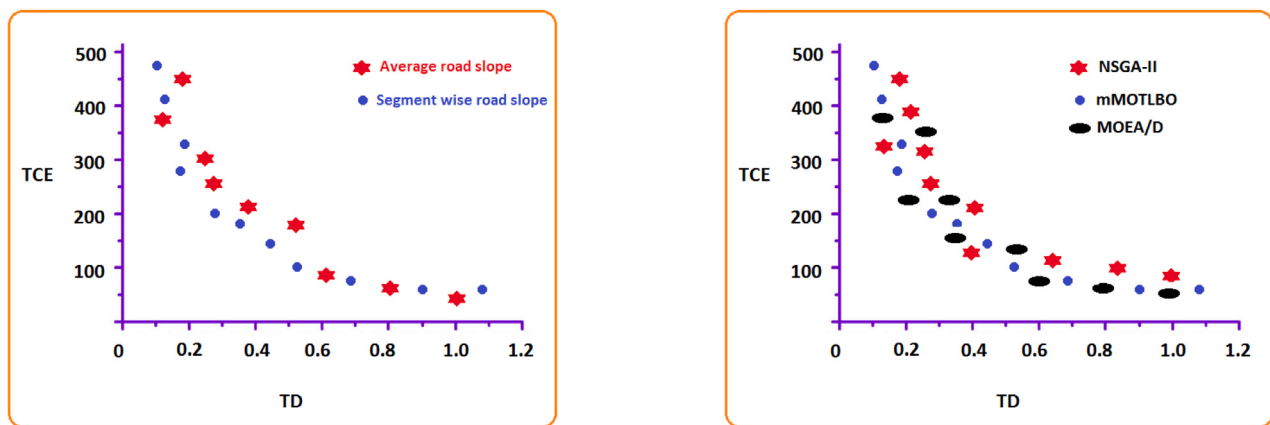


Fig. 18. Segment wise vs average road slope.

Fig. 19. Pareto front of proposed model.

Here, it is observed that for equal weights to both TCE and TCDS, the 7th solution ( $TCE = 197.34, TCDS = 0.31$ ) is the most preferable

one. In two extreme cases, for TCE having the lowest and highest importance, the respective preferred solutions are 11th and 4th.

**Table 9**

Results of the model A.

OS node[path] <i>velocity</i>	Optimum path node[path]	TCE	TD	Total Distance (KM)	Fuel cost (INR)	Fixed Carrying Charge (INR)	Goods Cost (INR)	Fixed Unloading Cost (INR)	Penalty Cost (INR)	Total Cost (INR)	Traveling Time (HR)	Fixed Time (HR)	Unloading Time (HR)	Land slide Recover (HR)	Total Time (HR)	
											(INR)	(INR)	(INR)	(HR)	(HR)	
1	1[0] <u>33.78</u> 3[1] <u>28.28</u> 2[2] <u>26.74</u> 10[2] <u>21.37</u> 9[1] <u>32.59</u> 5[2] <u>27.38</u> 6[2] <u>21.29</u> 8[2] <u>31.37</u> 7[1] <u>25.27</u> 4[0] <u>33.78</u> 1	10315.14	14800	40973.68	416	4000	2016	72520.82	5.98	0.11	3.33	2.69	12.11			
2	1[1] <u>21.23</u> 9[1] <u>26.17</u> 10[0] <u>21.87</u> 8[2] <u>27.31</u> 7[1] <u>26.74</u> 5[2] <u>32.33</u> 6[0] <u>28.74</u> 3[1] <u>26.11</u> 4[2] <u>34.19</u> 2[1] <u>31.34</u> 1	69.81	0.91	118	9870.20	14500	42827.56	650	4000	2335	74182.76	5.48	0.25	3.33	2.39	11.45
3	1[2] <u>26.87</u> 2[1] <u>24.23</u> 4[1] <u>31.27</u> 3[0] <u>25.87</u> 5[2] <u>34.29</u> 6[0] <u>27.38</u> 7[1] <u>27.29</u> 8[1] <u>24.58</u> 9[1] <u>31.28</u> 10[2] <u>29.38</u> 1	88.45	0.69	121	9744.30	14400	45656.04	812	4000	2520	77132.34	4.86	0.33	3.33	1.95	10.47
4	1[0] <u>18.35</u> 3[2] <u>22.34</u> 2[0] <u>31.98</u> 4[2] <u>28.56</u> 9[1] <u>22.34</u> 5[0] <u>21.42</u> 6[2] <u>32.69</u> 8[2] <u>24.56</u> 7[2] <u>18.27</u> 10[0] <u>21.57</u> 1	101.34	0.53	117	11622.46	14600	38048.38	735	4000	2714	71719.84	5.32	0.12	3.33	2.09	10.86
5	1[1] <u>22.37</u> 6[2] <u>19.37</u> 2[0] <u>28.24</u> 10[2] <u>26.37</u> 4[1] <u>19.83</u> 3[0] <u>32.87</u> 5[2] <u>17.39</u> 8[1] <u>21.85</u> 7[2] <u>24.38</u> 9[0] <u>28.92</u> 1	147.12	0.48	115	10855.30	14700	32795.02	440	4000	2084	64874.32	5.49	0.32	3.33	3.20	12.34
6	1[1] <u>18.23</u> 7[1] <u>22.74</u> 10[1] <u>33.98</u> 9[0] <u>15.28</u> 8[1] <u>34.78</u> 5[2] <u>22.69</u> 6[2] <u>19.63</u> 3[2] <u>22.38</u> 4[1] <u>16.85</u> 2[2] <u>29.37</u> 1	188.72	0.38	119	11135.43	14550	46209.98	620	4000	2117	78632.41	5.29	0.14	3.33	2.81	11.57
7	1[1] <u>32.85</u> 4[1] <u>31.79</u> 7[1] <u>26.54</u> 8[1] <u>23.59</u> 5[0] <u>19.85</u> 6[2] <u>21.53</u> 10[1] <u>31.25</u> 2[1] <u>33.87</u> 3[1] <u>22.37</u> 9[2] <u>28.68</u> 1	197.34	0.31	131	10387.67	14750	42680.10	890	4000	2439	75146.77	5.19	0.35	3.33	2.45	11.32
8	1[0] <u>19.84</u> 2[0] <u>22.84</u> 4[0] <u>19.73</u> 6[0] <u>33.67</u> 5[0] <u>34.79</u> 8[0] <u>31.42</u> 7[0] <u>21.57</u> 3[0] <u>20.98</u> 9[0] <u>19.56</u> 10[0] <u>27.49</u> 1	278.56	0.24	134	12618.37	14650	33758.76	720	4000	2610	68357.13	5.45	0.13	3.33	2.00	10.91
9	1[2] <u>24.78</u> 5[0] <u>33.85</u> 9[2] <u>22.58</u> 10[1] <u>21.37</u> 2[1] <u>23.96</u> 3[0] <u>25.94</u> 6[1] <u>19.37</u> 8[1] <u>15.27</u> 4[1] <u>21.69</u> 7[2] <u>33.74</u> 1	335.38	0.19	126	12242.86	14450	37842.59	975	4000	2117	71627.45	5.07	0.34	3.33	3.29	12.03
10	1[1] <u>22.34</u> 5[2] <u>34.39</u> 10[0] <u>21.87</u> 9[1] <u>19.37</u> 3[2] <u>20.84</u> 2[1] <u>24.67</u> 7[1] <u>23.96</u> 8[0] <u>25.84</u> 4[1] <u>30.67</u> 6[1] <u>31.86</u> 1	415.19	0.15	133	11912.14	14750	35795.73	670	4000	2336	69463.87	5.13	0.22	3.33	2.58	11.26
11	1[0] <u>16.93</u> 3[0] <u>18.56</u> 10[1] <u>32.97</u> 8[1] <u>31.27</u> 5[0] <u>19.73</u> 9[2] <u>21.67</u> 6[1] <u>33.52</u> 4[0] <u>31.54</u> 7[2] <u>23.57</u> 2[1] <u>11.29</u> 1	486.34	0.11	129	11722.24	14600	39687.20	430	4000	2685	73124.44	4.88	0.10	3.33	2.05	10.36

**Table 10**  
Optimum routing plan with TCE, TCDS, total cost and time with single path.

TCE	TCDS	Total cost	Total time	Optimum Route
88.57	1.19	76352.54	12.34	1[0]-6[0]-3[0]-2[0]-5[0]-4[0]-10[0]-8[0]-9[0]-7[0]-1
102.34	0.97	79812.27	11.89	1[0]-10[0]-3[0]-7[0]-6[0]-4[0]-5[0]-9[0]-8[0]-2[0]-1
144.86	0.78	81815.23	11.48	1[0]-3[0]-6[0]-5[0]-2[0]-4[0]-10[0]-8[0]-7[0]-9[0]-1
189.92	0.52	79391.12	11.85	1[0]-9[0]-8[0]-5[0]-4[0]-2[0]-10[0]-6[0]-7[0]-3[0]-1
199.65	0.43	64146.75	12.88	1[0]-7[0]-9[0]-2[0]-5[0]-10[0]-4[0]-8[0]-3[0]-6[0]-1
251.34	0.32	71456.31	12.47	1[0]-9[0]-7[0]-10[0]-4[0]-5[0]-2[0]-8[0]-3[0]-6[0]-1
352.87	0.27	85378.94	11.98	1[0]-6[0]-2[0]-10[0]-5[0]-4[0]-8[0]-3[0]-9[0]-7[0]-1
499.12	0.21	77815.23	12.16	1[0]-7[0]-9[0]-2[0]-5[0]-10[0]-4[0]-8[0]-3[0]-6[0]-1

**Table 11**  
Ranking by TOPSIS.

OS	Weighted value (TCE,TCDS)										
	TCE	TCDS	(0.1,0.9)	(0.2,0.8)	(0.3,0.7)	(0.4,0.6)	(0.5,0.5)	(0.6,0.4)	(0.7,0.3)	(0.8,0.2)	(0.9,0.1)
1	67.34	1.10	11	11	11	11	11	8	7	5	4
2	69.81	0.91	10	10	10	10	9	6	4	3	2
3	88.45	0.69	9	9	9	9	7	5	2	2	1
4	101.34	0.53	8	8	8	7	3	1	1	1	3
5	147.12	0.48	7	7	7	5	4	2	3	4	5
6	188.72	0.38	6	6	5	3	2	4	5	6	6
7	197.34	0.31	5	5	2	1	1	3	6	7	7
8	278.56	0.31	4	2	1	2	5	7	8	8	8
9	335.38	0.19	3	1	3	4	6	9	9	9	9
10	415.19	0.15	2	3	4	6	8	10	10	10	10
11	486.34	0.11	1	4	6	8	10	11	11	11	11

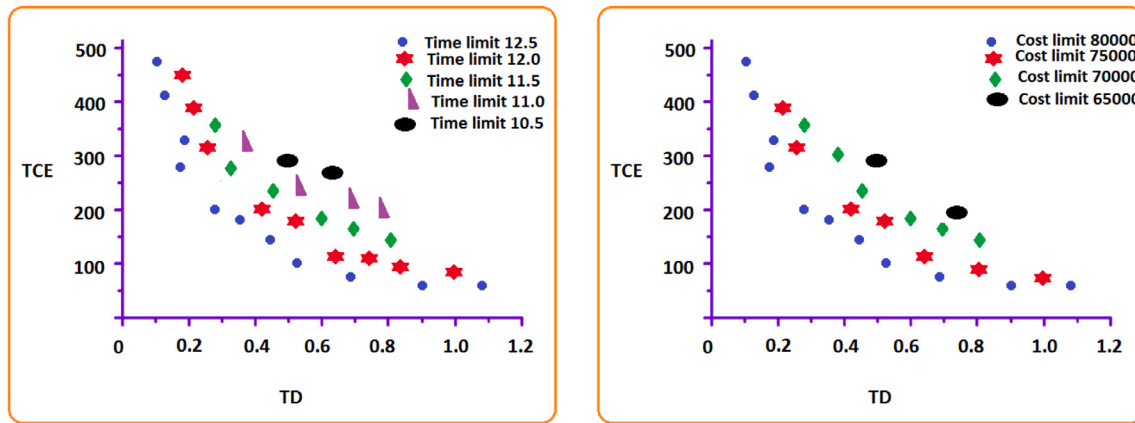


Fig. 20. Pareto front for time and cost limit.

#### 6.4.3. Results of Models-B, C, and D

Table 12 furnishes the feasible solutions of Models-B, C and D with multipath under respective constraints. These results of Models-B and -C are depicted in Figs. 20(a) and 20(b) respectively. The maximum time and cost of Models-B and C are 10.5 h and INR 65000 respectively. For Model-D, these limits are imposed jointly as 11.5 h and INR 65000. It is to be noted that, the single path ('0') formulations do not give any feasible solutions for Models-B, C and D after certain constraint values, though multipath gives results. So, it is again established that the use of the multipath model gives better solutions than the single-path model.

#### 7. Managerial insight

In Table 13, we present the managerial decisions (to opt out of the optimum results) in question-and-answer forms.

#### 8. Conclusion

##### 8.1. General conclusions

In this paper, a new algorithm for multi-objective problems, called mMOTLBO is proposed and illustrated. mMOTLBO is also tested with some test problems from TSPLIB and compared with true Pareto front from NSGA-II, MOEA/D and mNSGA-II. In mMOTLBO, with Boltzmann selection, a novel up-gradation strategy in the teaching phase, and interactive group-based crossover for learners in the learning phase, along with the self-learning phase are introduced after both teaching and learning phases. Here, the development of mMOTLBO is in general form and it can be applied to other discrete problems such as network optimization, vehicle routing, VLSI chip design, procurement planning, facility location problem, disaster management problem, etc.

**Table 12**  
Optimum results of TCE, TD, with time and cost constraints.

	Time limit	Multipath			Without multipath				
		Cost limit	TCE	TCDS	Total cost	Total time	TCE	TD	Total cost
Model B	12.5	67.34	1.10	72 520.82		88.57	1.19	76 352.54	
		69.81	0.91	74 182.76		102.34	0.97	79 812.27	
		88.45	0.69	77 132.34		144.86	0.78	81 815.23	
	12.0	99.03	1.02	76 856.76		102.34	0.92	79 812.27	
		103.34	0.88	77 980.41		189.92	0.87	81 398.76	
		122.89	0.77	79 146.77		199.65.87	0.81	85 378.94	
	11.5	152.43	0.83	79 658.87		185.86	0.76	87 459.82	
		173.13	0.71	81 823.54		206.65	0.63	90 548.65	
		194.67	0.59	81 980.24		225.62	0.59	95 486.44	
	11.0	202.76	0.81	83 429.31		—	NFS	—	
		226.54	0.73	85 681.56		—	NFS	—	
		251.98	0.54	88 453.90		—	NFS	—	
	10.5	278.70	0.65	91 908.54		—	NFS	—	
		298.36	0.53	94 387.71		—	NFS	—	
	10.0	—	NFS	—		—	NFS	—	
Model C	80 000	67.34	1.10		12.11	88.57	1.19	12.34	
		69.81	0.91		11.45	102.34	0.97	11.89	
		88.45	0.69		10.47	144.86	0.78	11.48	
		75 000	87.56	1.11	12.43	152.53	0.72	11.32	
		98.32	0.83		11.56	165.34	0.67	11.06	
	70 000	101.34	0.53		10.80	—	NFS	—	
		127.54	0.82		10.91	199.65	0.43	12.88	
		175.98	0.71		10.26	—	NFS	—	
		196.36	0.63		10.04	—	NFS	—	
		65 000	199.52	0.79	10.01	—	NFS	—	
	60 000	278.65	0.51		9.89	—	NFS	—	
		NFS	—		—	—	NFS	—	
Model D	12.5	80 000	67.34	1.10		88.57	1.19		
		69.81	0.91		102.34	0.97			
		88.45	0.69		144.86	0.78			
	12.0	75 000	73.23	0.96		148.52	0.74		
		89.82	0.81		—	NFS			
	11.5	97.33	0.65		—	NFS			
		70 000	112.56	0.62	—	NFS			
	11.0	65 000	NFS	—	—	NFS			

**Table 13**  
Research questions, solutions and managerial insight.

Research Questions	Solutions (with reference)	Managerial insight
Q1: How to choose the appropriate routing path for minimum carbon emission and customer dissatisfaction?		Management can make the appropriate decision to select the supplier.
How logistic routing perform to reduce the carbon emission?	Tables 9, 10 and Fig. 19	Management can endeavor to decrease carbon emissions.
How logistic routing perform to reduce the customer's dissatisfaction?		Management should make efforts to minimize customer dissatisfaction.
Q2: How road gradient impact on the carbon emission and routing?	Table 9, and Fig. 3(a)	Carbon emissions are determined by both distance traveled and road gradient.
Q3: How multipath impact on routing and solution space?	Tables 9 and 10, and Fig. 17(b)	It is observed that multipath better than single path
Q4: How to formulate the multi-objective problem with cost or/and time constraints?	Table 12, and Figs. 20(a), 20(b)	For this investigation, results of multi-objective with constraints are obtained.
Q5: How to address the penalty due to customer dissatisfaction?	Table 9 and 12 and Fig. 5	Retailer operating time different, penalty can be handled through these models.
Q6: How to address the landslide recover time?	Table 9 and 12 and Fig. 3(b)	Road condition varies in different path landslide also.
Q7: How to solve these problems using MOTLBO?	Table 9, and Fig. 19	For this investigation, introduce problem-specific mMOTLBO.

Thus, the contributions of the present investigation are twofold: (i) development of a real-life delivery problem (a green multi-objective 3D delivery problem with customer dissatisfaction in the hilly region to simultaneously reduce the overall CE and CDS) considering road gradient, carbon emission, customer dissatisfaction, multipath, landslide recover time, etc., and (ii) development of mMOTLBO with probabilistic selection, a novel up-gradation strategy in the teaching phase, and interactive group-based crossover for learners in the learning phase, along with a self-learning phase introduced after both the teaching and learning phases. The validity and supremacy of mMOTLBO are established through the different multi-objective test functions, such as ONVG, OTNVG, OTNVGR, ER, IGD, GD, Spread, HV, etc. The following are the specific numerical advantages of the proposed mMOTLBO over other algorithms. (i) Performance metrics: The proposed mMOTLBO achieved significant improvements in ONVG, OTNVG, OTNVGR compared to NSGA-II and MOEA/D, with 82, 76, and 92.68%, respectively. (ii) Real-life problem application: The SMO3DDPwCS problem solved using mMOTLBO resulted in practical gains, such as a reduction in CE (499.12 to 88.57) and improvement in CDS (0.21 to 1.19), demonstrating the algorithm's real-world relevance.

## 8.2. Limitations and future scope

The limitations of the present investigation are (i) only one vehicle is considered for delivery (routing) due to resource constraints, (ii) the capacity of the vehicle is considered large enough to accommodate the demands of all retailers. It may be taken of finite capacity, (iii) MOTLBO is applied here for a small-scale problem of  $(10 \times 3)$  size.

In future, (i) Models with different imprecise parameters (fuzzy, rough, random, etc.) can also be formulated and solved, (ii) different discrete multi-objective optimization problems in other areas such as TPP, VRP, etc. can be formulated and solved by mMOTLBO. It also be used to minimize the cost and time under different carbon policy-tax, cap, and trade.

## CRediT authorship contribution statement

**Somnath Maji:** Writing – review & editing, Writing – original draft, Visualization, Supervision, Software, Methodology, Investigation, Formal analysis, Data curation, Conceptualization. **Samir Maity:** Writing – original draft, Validation, Software, Methodology, Investigation, Data curation, Conceptualization. **Izabela Ewa Nielsen:** Writing – review & editing, Validation, Supervision, Investigation. **Debasis Giri:** Supervision. **Manoranjan Maiti:** Writing – review & editing, Validation, Supervision, Methodology, Investigation, Data curation, Conceptualization.

## Code availability

System: Windows 2010, CPU: CORE i5, RAM: 4 GB, Software: C++ (Code Block), MATLAB.

## Ethics approval

This article does not contain any studies with human participants or animals performed by any of the authors.

## Funding

No funding was received for conducting this study.

## Declaration of competing interest

We have no conflict of interest, mention all funding agencies and agree with the journal publishing ethics and rules.

## Data availability

Data will be made available on request.

## References

- [1] K. Obaideen, M.A. Abdulkareem, T. Wilberforce, K. Elsaied, E.T. Sayed, H.M. Maghrabie, A. Olabi, Biogas role in achievement of the sustainable development goals: Evaluation, Challenges, and Guidelines, *J. Taiwan Inst. Chem. Eng.* 131 (2022) 104207.
- [2] A.A.R.N. Avotra, A. Nawaz, Asymmetric impact of transportation on carbon emissions influencing SDGs of climate change, *Chemosphere* 324 (2023) 138301.
- [3] M. Xu, Z. Qin, How does vehicle emission control policy affect air pollution emissions? Evidence from Hainan Province, China, *Sci. Total Environ.* 866 (2023) 161244.
- [4] N. Elgarably, S. Easa, A. Nassef, A. El Damatty, Stochastic multi-objective vehicle routing model in green environment with customer satisfaction, *IEEE Trans. Intell. Transp. Syst.* 24 (1) (2022) 1337–1355.
- [5] P. Fan, G. Song, Z. Zhu, Y. Wu, Z. Zhai, L. Yu, Road grade estimation based on large-scale fuel consumption data of connected vehicles, *Transp. Res. Part D: Transp. Environ.* 106 (2022) 103262.
- [6] S. Maji, K. Pradhan, S. Maity, I.E. Nielsen, D. Giri, M. Maiti, Emergent multipath COVID-19 specimen collection problem with green corridor through variable length GA, *Expert Syst. Appl.* (2023) 120879.
- [7] K. Thakur, S. Maji, S. Maity, T. Pal, M. Maiti, Multiroute fresh produce green routing models with driver fatigue using Type-2 fuzzy logic-based DFWA, *Expert Syst. Appl.* 229 (2023) 120300.
- [8] D. Lei, B. Su, A multi-class teaching-learning-based optimization for multi-objective distributed hybrid flow shop scheduling, *Knowl.-Based Syst.* (2023) 110252.
- [9] S. Maji, S. Mondal, S. Maity, D. Giri, M. Maiti, A modified teaching-learning-based optimization algorithm for traveling salesman problem, in: *Human-Centric Smart Computing: Proceedings of ICHCSC 2022*, Springer, 2022, pp. 293–303.
- [10] G. Reinelt, *Tsplib95*, Interdisziplinäres Zentru Für Wissenschaft Rechnen (IWR), Heidelberg 338 (1995).
- [11] S. Sabet, B. Farooq, Green vehicle routing problem: State of the art and future directions, *IEEE Access* (2022).
- [12] G.J. Micheli, F. Mantella, Modelling an environmentally-extended inventory routing problem with demand uncertainty and a heterogeneous fleet under carbon control policies, *Int. J. Prod. Econ.* 204 (2018) 316–327.
- [13] O. Golbasi, E. Kina, Haul truck fuel consumption modeling under random operating conditions: A case study, *Transp. Res. Part D: Transp. Environ.* 102 (2022) 103135.
- [14] G. Scora, M. Barth, Comprehensive modal emissions model (cmem), version 3.01, in: User Guide. Centre for Environmental Research and Technology, 1070, University of California, Riverside, 2006.
- [15] T. Bektaş, G. Laporte, The pollution-routing problem, *Transp. Res. Part B: Methodol.* 45 (8) (2011) 1232–1250.
- [16] S.E. Comert, H.R. Yazgan, A new approach based on hybrid ant colony optimization-artificial bee colony algorithm for multi-objective electric vehicle routing problems, *Eng. Appl. Artif. Intell.* 123 (2023) 106375.
- [17] B.K. Giri, S.K. Roy, Neutrosophic multi-objective green four-dimensional fixed-charge transportation problem, *Int. J. Mach. Learn. Cybern.* 13 (10) (2022) 3089–3112.
- [18] X. Ren, X. Jiang, L. Ren, L. Meng, A multi-center joint distribution optimization model considering carbon emissions and customer satisfaction, *Math. Biosci. Eng.* 20 (2023) 683–706.
- [19] S. Wang, X. Wang, X. Liu, J. Yu, A bi-objective vehicle-routing problem with soft time windows and multiple depots to minimize the total energy consumption and customer dissatisfaction, *Sustainability* 10 (11) (2018) 4257.
- [20] X. Wang, X. Sun, J. Dong, M. Wang, J. Ruan, Optimizing terminal delivery of perishable products considering customer satisfaction, *Math. Probl. Eng.* 2017 (2017).
- [21] R. Liu, T. Yang, G. Sun, S. Lin, F. Li, X. Wang, Multi-objective optimal scheduling of community integrated energy system considering comprehensive customer dissatisfaction model, *IEEE Trans. Power Syst.* (2022).
- [22] I. Wijaya, A. Joshi, M. Alam, S. Jayasinghe, N. Laila, Climate change induced landslide susceptibility assessment-for aiding climate resilient planning for road infrastructure: A case study in Rangamati District, Chittagong Hill Tracts, Bangladesh, in: *IOP Conference Series: Earth and Environmental Science*, 1091, (1) IOP Publishing, 2022, 012010.
- [23] B. Hafsa, M.S. Chowdhury, M.N. Rahman, Landslide susceptibility mapping of Rangamati District of Bangladesh using statistical and machine intelligence model, *Arab. J. Geosci.* 15 (15) (2022) 1367.
- [24] H. Chen, C. Lee, A dynamic model for rainfall-induced landslides on natural slopes, *Geomorphology* 51 (4) (2003) 269–288.
- [25] V.S. Khoroshilov, A.P. Karpik, I.A. Musikhin, Mathematical modeling of landslide slope dynamics and sustainable development of territories of Asian Russia, 2021, Peprint Version.

- [26] A. Ben-Said, A. Moukrim, R.N. Guibadj, J. Verny, Using decomposition-based multi-objective algorithm to solve Selective Pickup and Delivery Problems with Time Windows, *Comput. Oper. Res.* 145 (2022) 105867.
- [27] Y. Lu, C. Yang, J. Yang, A multi-objective humanitarian pickup and delivery vehicle routing problem with drones, *Ann. Oper. Res.* 319 (1) (2022) 291–353.
- [28] P. Ghasemi, H. Hemmati, A. Pourghader Chobar, M.R. Heidari, M. Keramati, A multi-objective and multi-level model for location-routing problem in the supply chain based on the customer's time window, *J. Appl. Res. Ind. Eng.* (2022).
- [29] X.-R. Tao, Q.-K. Pan, H.-Y. Sang, L. Gao, A.-L. Yang, M. Rong, Nondominated sorting genetic algorithm-II with Q-learning for the distributed permutation flowshop rescheduling problem, *Knowl.-Based Syst.* 278 (2023) 110880.
- [30] C. Liu, L. Wu, W. Xiao, G. Li, D. Xu, J. Guo, W. Li, An improved heuristic mechanism ant colony optimization algorithm for solving path planning, *Knowl.-Based Syst.* 271 (2023) 110540.
- [31] H. Luo, W. Xu, Y. Tan, A discrete fireworks algorithm for solving large-scale travel salesman problem, in: 2018 IEEE Congress on Evolutionary Computation, CEC, IEEE, 2018, pp. 1–8.
- [32] J.-w. Zhang, W.-j. Si, Improved enhanced self-tentative PSO algorithm for TSP, in: 2010 Sixth International Conference on Natural Computation, vol. 5, IEEE, 2010, pp. 2638–2641.
- [33] R.V. Rao, V.J. Savsani, D. Vakharia, Teaching-learning-based optimization: a novel method for constrained mechanical design optimization problems, *Comput.-Aided Des.* 43 (3) (2011) 303–315.
- [34] R. Rao, Review of applications of TLBO algorithm and a tutorial for beginners to solve the unconstrained and constrained optimization problems, *Decis. Sci. Lett.* 5 (1) (2016) 1–30.
- [35] Y. Xu, Z. Yang, X. Li, H. Kang, X. Yang, Dynamic opposite learning enhanced teaching-learning-based optimization, *Knowl.-Based Syst.* 188 (2020) 104966.
- [36] J.-q. Li, Q.-k. Pan, K. Mao, A discrete teaching-learning-based optimisation algorithm for realistic flowshop rescheduling problems, *Eng. Appl. Artif. Intell.* 37 (2015) 279–292.
- [37] S.D.K. Ram, S. Srivastava, K. Mishra, A multi-objective generalized teacher-learning-based-optimization algorithm, *J. Inst. Eng. (India): Ser. B* 103 (5) (2022) 1415–1430.
- [38] D. Li, C. Zhang, X. Shao, W. Lin, A multi-objective TLBO algorithm for balancing two-sided assembly line with multiple constraints, *J. Intell. Manuf.* 27 (2016) 725–739.
- [39] N.-C. Yang, S.-W. Liu, Multi-objective teaching-learning-based optimization with pareto front for optimal design of passive power filters, *Energies* 14 (19) (2021) 6408.
- [40] D. Chen, F. Zou, R. Lu, L. Yu, Z. Li, J. Wang, Multi-objective optimization of community detection using discrete teaching-learning-based optimization with decomposition, *Inform. Sci.* 369 (2016) 402–418.
- [41] J.C. Molina, I. Eguia, J. Racero, F. Guerrero, Multi-objective vehicle routing problem with cost and emission functions, *Procedia- Soc. Behav. Sci.* 160 (2014) 254–263.
- [42] S. Iqbal, M. Kaykobad, M.S. Rahman, Solving the multi-objective vehicle routing problem with soft time windows with the help of bees, *Swarm Evol. Comput.* 24 (2015) 50–64.
- [43] E.M. Toro, J.F. Franco, M.G. Echeverri, F.G. Guimarães, A multi-objective model for the green capacitated location-routing problem considering environmental impact, *Comput. Ind. Eng.* 110 (2017) 114–125.
- [44] M.A. Eirgash, V. Togan, T. Dede, A multi-objective decision making model based on TLBO for the time-cost trade-off problems, *Struct. Eng. Mech.* 71 (2) (2019) 139–151.
- [45] W. Liao, L. Zhang, Z. Wei, Multi-objective green meal delivery routing problem based on a two-stage solution strategy, *J. Clean. Prod.* 258 (2020) 120627.
- [46] S. Zajac, S. Huber, Objectives and methods in multi-objective routing problems: a survey and classification scheme, *European J. Oper. Res.* 290 (1) (2021) 1–25.
- [47] F. Pilati, R. Tronconi, Multi-objective optimisation for sustainable few-to-many pickup and delivery vehicle routing problem, *Int. J. Prod. Res.* (2023) 1–30.
- [48] W. Chen, S. Zhang, R. Li, H. Shahabi, Performance evaluation of the GIS-based data mining techniques of best-first decision tree, random forest, and naïve Bayes tree for landslide susceptibility modeling, *Sci. Total Environ.* 644 (2018) 1006–1018.
- [49] H. Zhang, Y. Song, S. Xu, Y. He, Z. Li, X. Yu, Y. Liang, W. Wu, Y. Wang, Combining a class-weighted algorithm and machine learning models in landslide susceptibility mapping: A case study of Wanzhou section of the Three Gorges Reservoir, China, *Comput. Geosci.* 158 (2022) 104966.
- [50] D. Maraun, R. Knevels, A.N. Mishra, H. Truhetz, E. Bevacqua, H. Proske, G. Zappa, A. Brenning, H. Petschko, A. Schaffer, et al., A severe landslide event in the Alpine foreland under possible future climate and land-use changes, *Commun. Earth Environ.* 3 (1) (2022) 87.
- [51] S. Maity, A. Roy, M. Maiti, An imprecise multi-objective genetic algorithm for uncertain constrained multi-objective solid travelling salesman problem, *Expert Syst. Appl.* 46 (2016) 196–223.
- [52] K. Deb, S. Agrawal, A. Pratap, T. Meyarivan, A fast elitist non-dominated sorting genetic algorithm for multi-objective optimization: NSGA-II, in: Parallel Problem Solving from Nature PPSN VI: 6th International Conference Paris, France, September 18–20, 2000 Proceedings 6, Springer, 2000, pp. 849–858.
- [53] S. Maity, A. Roy, M. Maiti, A modified genetic algorithm for solving uncertain constrained solid travelling salesman problems, *Comput. Ind. Eng.* 83 (2015) 273–296.
- [54] J. Gottlieb, G.R. Raidl, Evolutionary Computation in Combinatorial Optimization: 6th European Conference, EvoCOP 2006, Budapest, Hungary, April 10–12, 2006, Proceedings, vol. 3906, Springer, 2006.
- [55] I. Khan, K. Basuli, M.K. Maiti, Multi-objective covering salesman problem: a decomposition approach using grey wolf optimization, *Knowl. Inf. Syst.* 65 (1) (2023) 281–339.
- [56] J. Bigeon, S. Le Digabel, L. Salomon, DMulti-MADS: Mesh adaptive direct multisearch for bound-constrained blackbox multiobjective optimization, *Comput. Optim. Appl.* 79 (2) (2021) 301–338.
- [57] I. Khan, M.K. Maiti, K. Basuli, Multi-objective traveling salesman problem: an ABC approach, *Appl. Intell.* 50 (2020) 3942–3960.
- [58] Q. Liu, X. Li, H. Liu, Z. Guo, Multi-objective metaheuristics for discrete optimization problems: A review of the state-of-the-art, *Appl. Soft Comput.* 93 (2020) 106382.
- [59] S. Dhouib, A. Kharraf, T. Loukil, H. Chabchoub, Enhancing the dhouib-matrix-4 metaheuristic to generate the Pareto non-dominated set solutions for multi-objective travelling salesman problem: The DM4-PMO method, *Results Control Optim.* 14 (2024) 100402.
- [60] A. Agrawal, N. Ghune, S. Prakash, M. Ramteke, Evolutionary algorithm hybridized with local search and intelligent seeding for solving multi-objective Euclidian TSP, *Expert Syst. Appl.* 181 (2021) 115192.
- [61] J. Shi, J. Sun, Q. Zhang, Multi-objectivization inspired metaheuristics for the sum-of-the-parts combinatorial optimization problems, *Appl. Soft Comput.* 103 (2021) 107157.
- [62] I. Khan, M.K. Maiti, K. Basuli, Multi-objective generalized traveling salesman problem: a decomposition approach, *Appl. Intell.* 52 (10) (2022) 11755–11783.
- [63] S. Opricovic, G.-H. Tzeng, Compromise solution by MCDM methods: A comparative analysis of VIKOR and TOPSIS, *European J. Oper. Res.* 156 (2) (2004) 445–455.
- [64] S. Ghosh, S.K. Roy, Closed-loop multi-objective waste management through vehicle routing problem in neutrosophic hesitant fuzzy environment, *Appl. Soft Comput.* (2023) 110854.